
**Hydrocarbon kitchen evolution of the Lower Silurian Longmaxi Formation in the Sichuan Basin of China and its contribution to shale gas and natural gas accumulation**

Jia–zhen Zhang, Chang–cheng Wang, Yin–hui Zuo, Xin–guo Duan, Wen–ming Huang, Mei–hua Yang, Jian–cheng Zeng

**Citation:** Jia–zhen Zhang, Chang–cheng Wang, Yin–hui Zuo, Xin–guo Duan, Wen–ming Huang, Mei–hua Yang, Jian–cheng Zeng, 2025. Hydrocarbon kitchen evolution of the Lower Silurian Longmaxi Formation in the Sichuan Basin of China and its contribution to shale gas and natural gas accumulation, China Geology, 8, 1–19. doi: 10.31035/cg20240143.

View online: http://www.jos.ac.cn/article/shaid/a323477d45d5271f07a3b090b2f508dc3702cd8c4cf394020105f01e7dd91987

---

China Geology 8 (2025) 1−19

China Geology

Journal homepage: http://chinageology.cgs.cn
https://www.sciencedirect.com/journal/china-geology

# Hydrocarbon kitchen evolution of the Lower Silurian Longmaxi Formation in the Sichuan Basin of China and its contribution to shale gas and natural gas accumulation

Jia-zhen Zhang[a, b], Chang-cheng Wang[a,*], Yin-hui Zuo[a, b], Xin-guo Duan[a], Wen-ming Huang[c], Mei-hua Yang[a, b], Jian-cheng Zeng[a, b]

[a] *State Key Laboratory of Oil and Gas Reservoir Geology and Exploitation*, *Chengdu University of Technology*, *Chengdu* 610059, *China*
[b] *Tianfu Yongxing Laboratory*, *Chengdu*, 610217, *China*
[c] *Sulige Project Management Department*, *CNPC Chuanqing Drilling Engineering Company Limited*, 610051, *China*

ARTICLE INFO

*Article history:*
Received 4 July 2024
Received in revised form 10 November 2024
Accepted 6 December 2024
Available online 29 April 2025

*Keywords:*
Oil and gas exploration engineering
Hydrocarbon kitchen evolution
Maturity history
Hydrocarbon generation history
Shale gas accumulation
Basin modeling technology
Sichuan Basin
Longmaxi Formation

ABSTRACT

The Lower Silurian Longmaxi Formation has been proven to be an important source rock in the Sichuan Basin, which not only provides gas from conventional natural gas reservoirs, but also forms shale gas reservoirs. On the basis of the tectono-thermal history, basin modeling technology was used to restore the evolution of hydrocarbon kitchens and further identify favorable areas for gas exploration. The results revealed that the Longmaxi Formation experienced two stages of hydrocarbon generation, corresponding to the formation of three hydrocarbon kitchens, all of which generated mainly oil, with natural gas as a supplement. During the early stage of the early Yanshan Movement, the generated oil and gas migrated to the high parts of the paleo-uplifts to form the Luzhou and Kaijiang paleo-oil reservoirs. With increasing burial depth and formation temperature, the oil in paleo-oil reservoirs was cracked into natural gas, which was mixed with the natural gas generated by late kerogen, then adjusted by complex tectonic movements and finally formed both natural gas and shale gas reservoirs. The two paleo-oil reservoir development locations and their surroundings are potential areas of conventional gas and shale gas reservoirs. Future exploration efforts should focus on the two paleo-oil reservoirs and their surroundings.



## 1. Introduction

With the proposal of the carbon peak and carbon neutrality actions, global energy is shifting from high carbon to low carbon (Agyeman SD and Lin BQ, 2023; Moghaddam H and Kunst RM, 2023). Natural gas has the advantages of flexibility, safety, and cleanliness. It is indispensable for the global net-zero emission process (da Silva VO et al., 2023; Smit DJ et al., 2023; Hou ZY et al., 2024). The Sichuan Basin is one of the earliest sizeable natural gas-rich basins that has been used to develop and supply energy from natural gas in the world (Yang Z et al., 2022; Zhang NN et al., 2024). Large-scale oil and gas exploration and development in the Sichuan Basin began in the 1950s. After continuous exploration efforts, natural gas production in the Sichuan Basin exceeded $565.0\times10^8$ $m^3$ in 2021, accounting for 25% of China´s natural gas production (Wei GQ et al., 2022; Zhang JZ et al., 2023). According to the fourth oil and gas resources evaluation by PetroChina, the natural gas geological resources in the Sichuan Basin are $38.18\times10^{12}$ $m^3$, with a proven rate of only 10% (Liu SG et al., 2020; Zheng ZY et al., 2023). Compared with most large oil and gas basins in the world (with a proven rate of 60% in the Permian Basin (Saputra W et al., 2021) and 44% in the Anadarko Basin (Fritz RD and Mitchell JR, 2021), the Sichuan Basin is still in the early-middle stage of exploration and has enormous potential for future exploration.

The natural gas in the Sichuan Basin mainly derived from the cracking of crude oil in paleo-oil reservoirs. The oil source of the paleo-oil reservoirs came from the source rocks in each reservoir (Liu SG et al., 2020; Huang SP et al., 2023; Zheng ZY et al., 2023). Hydrocarbon kitchens generally refer to mature source rock masses with high organic matter abundances, good properties, and great hydrocarbon

First author: *E-mail address*: 783707206@qq.com (Jiazhen Zhang).

* Corresponding author: *E-mail address*: wcc-126@163.com (Changcheng Wang).

Literary editor: Xi-jie Chen
doi:10.31035/cg20240143
2096-5192/© 2025 China Geology Editorial Office.

generation potential in the study area (Demaison G, 1984; Thomas BM et al., 1985; Evenick JC, 2023). Many oil and gas exploration analyses have shown that the previously discovered large- and medium-sized gas fields are closely related to the distribution of hydrocarbon kitchens and have characteristics of being located near hydrocarbon kitchens. The Xinchang, Puguang, Yuanba, Anyue and other large gas fields that have been discovered in the Sichuan Basin are all located in the hydrocarbon generation center and its surroundings (Ma XH et al., 2019; Evenick JC et al., 2023). Hydrocarbon kitchens are the most suitable method for characterizing the hydrocarbon generation centers of basins. Hydrocarbon kitchens and their surroundings are the main areas for forming paleo-oil reservoirs and are the critical areas for discovering large- and medium-sized gas fields (Pang XQ et al., 2015; Tian XW et al., 2020). In recent years, with the advancements in computer and seismic exploration technology, many scholars have used basin modeling technology to reveal the evolution of hydrocarbon kitchens in a particular area in combination with organic geochemical parameters, which has effectively guided petroleum geological exploration in related basin zones (Yang Z and Zou CN, 2019; Baniasad A et al., 2021; de Almeida dos Reis MAA et al., 2023; Shabani F et al., 2023).

After years of natural gas exploration and research, it has been confirmed that the source rock of the Lower Silurian Longmaxi Formation is the main source rock of the Silurian–Carboniferous gas-bearing system in the Sichuan Basin. This source rock not only provided natural gas for the conventional Carboniferous gas reservoirs but also formed the Longmaxi Formation shale gas reservoirs. At present, one large conventional gas field, namely, Datianchi, has been discovered in the eastern Sichuan Basin, as have 13 medium-sized conventional gas fields, such as the Dacigan, Qilixia, Wolonghe, and Gaofengchang gas fields. The proven geological reserves are $2351\times10^8$ $m^3$ (Wang K et al., 2016; Ma XH et al., 2019). Moreover, shale gas reservoirs in Fuling, Weiyuan, Weirong, Yongchuan, Changning, Wulong, Pengshui and Zhaotong have been discovered (He ZL et al., 2020; Wang YM et al., 2020; Nie HK et al., 2024). According to the prediction of the Strategic Research Center of Oil and Gas Resources of the Ministry of Land and Resources (2016), the geological resources of shale gas in China are $123.01\times10^{12}$ $m^3$, of which the Sichuan Basin and its surrounding areas represent $57.27\times10^{12}$ $m^3$. However, during conventional gas reservoir exploration efforts, only one large gas field, Datianchi, has been found in the Silurian–Carboniferous gas-bearing system at present. Are there any other large or extra-large gas fields? In addition, exploration for shale gas in the Longmaxi Formation is still in its infancy. Studying the basic characteristics of source rocks and hydrocarbon kitchen evolution is important for exploring the mechanism of conventional and shale gas accumulations and optimizing potential areas.

In the study of the Longmaxi Formation, scholars have focused on the static characteristics of the source rock, such as the source rock thickness (Hu ZQ et al., 2020; Wang YM et al., 2021), paleogeographic environment (Tian XW et al., 2020; Tang X et al., 2021), geochemical characteristics (Qi L et al., 2020; Xiao B et al., 2021; Wu B, 2022; Liu K and Zhang C, 2022; Chen L et al., 2023), and current hydrocarbon generation intensity (Ma XH et al., 2019; Guo XS et al., 2020). However, there is a lack of systematic research on the dynamic processes of the Longmaxi Formation, such as maturity, hydrocarbon generation history, and hydrocarbon kitchen evolution during geological time, which restricts the study of the dynamics of natural gas accumulations. The maturity evolution of the source rocks in the Sichuan Basin was controlled by the paleogeothermal field (Qiu NS et al., 2021). Restoring its maturity evolution and hydrocarbon generation history and clarifying the times, locations, and migration evolution of hydrocarbon kitchens are essential to research the natural gas accumulation patterns in such basins. Therefore, this paper takes the tectono-thermal history of the Sichuan Basin as a constraint, combines the geochemical parameters of the source rock, and uses basin modeling technology to restore the maturity evolution and hydrocarbon generation history of the Longmaxi Formation. It clarifies the times and locations of the formation of hydrocarbon kitchens, reveals the evolution features and resource scales of different hydrocarbon kitchens, and indicates the matching relationship between the hydrocarbon kitchens and gas accumulations. This work further reveals the potential paleo-oil reservoir areas and highlights favorable directions for gas exploration. This study provides not only basic parameters but also favorable support for conventional gas and shale gas exploration in the Sichuan Basin. However, this study also provides a reference method for the study of the evolution of hydrocarbon kitchens and the gas accumulation dynamics in other sedimentary basins.

## 2. Geological setting

### *2.1. Geological background of the Sichuan Basin*

The Sichuan Basin is located on the eastern Qinghai–Tibet Plateau and is geologically situated on the northwest edge of the Yangtze Plate, with an area of approximately $18 \times 10^4$ $km^2$. It is a superposition basin that has undergone a complex tectonic evolutionary process. It is surrounded by the Micang Mountains, Daba Mountains, Longmen Mountains, and Qiyue Mountains, forming a diamond-shaped distribution. The structure is characterized by multiple structural boundaries and systems that are controlled by various deep faults (Fig. 1; Liu SG et al., 2021; Zuo YH et al., 2024). The Sichuan Basin contains Sinian, Cambrian, Ordovician, Silurian, Carboniferous, Permian, Triassic, and Jurassic strata that were deposited from bottom to top, with large thicknesses and wide distributions (Fig. 2; Zuo YH et al., 2024). The Sinian to Middle Triassic strata are a marine sedimentary system that is composed mainly of carbonate rocks with a thickness of 4100–7000 m. The Upper Triassic strata are a marine–continental transitional facies deposit with a thickness

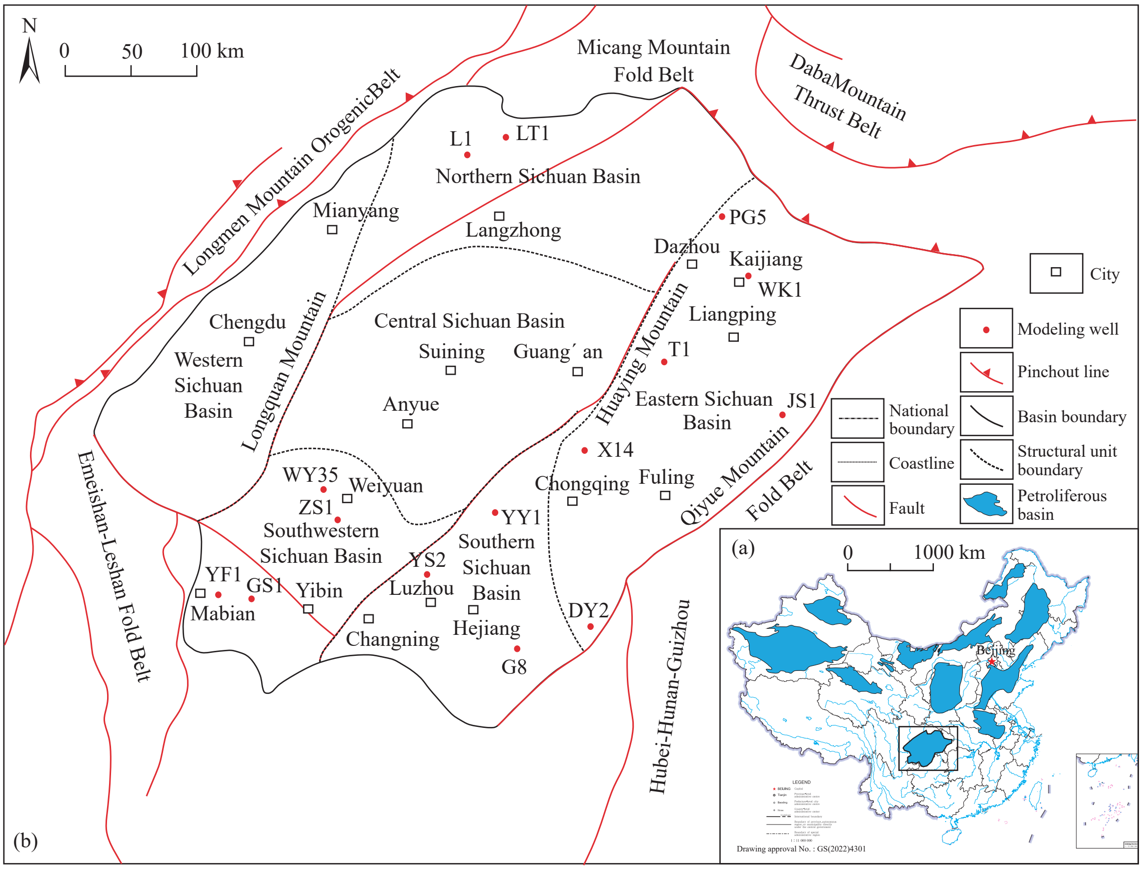


**Fig. 1.** Position and structural unit division of the Sichuan Basin (revised from Liu SG et al., 2021; Zuo YH et al., 2024). a–Position of the Sichuan Basin. b–Structural unit division of the Sichuan Basin.

of 250–3000 m. The Jurassic to Quaternary strata consist of continental deposits that have developed mainly terrestrial clastic rocks with a thickness of 2000–5000 m. Affected by the Caledonian Movement, most of the Upper Silurian, Devonian, and Lower Carboniferous strata are missing in the eastern Sichuan Basin. At the same time, only the Huanglong Formation remained in the Middle Carboniferous. Owing to the Yanshan–Himalayan Movement, the interval from the Middle Jurassic to Quaternary experienced different degrees of uplift and erosion (Ma XH et al., 2019; Liu SG et al., 2020, 2021).

## 2.2. Stratigraphic background of the Longmaxi Formation

The Lower Silurian Longmaxi Formation is a set of shallow to deep-water continental shelf strata, with black shale and dark gray mudstone rich in organic and siliceous matter and graptolites (Guo XS et al., 2020). Owing to erosion, the areas of exposed Silurian strata in the central and western parts of the basin are small or nonexistent, and the source rocks are not well developed (Liu SG et al., 2021). The source rocks are distributed mainly in the southern, eastern, and northern parts of the basin. The thickness of the source rocks varies from 0 to 100 m (revised from Hu ZQ et al., 2020; Wang YM et al., 2021). There are three high-value areas in the basin, namely, Kaijiang, Fuling, and Yibin-Luzhou, with thicknesses greater than 100 m. The distribution pattern generally consists of greater thicknesses in the southeast and thinner deposits in the northwest (Fig. 3). The total organic carbon content (TOC) ranges from 1.0% to 3.2% (revised from Hu ZQ et al., 2020; Wang YM et al., 2021) (Fig. 4). This organic carbon is primarily composed of lower aquatic organisms, and the kerogen is mainly type I, with a strong hydrocarbon generation ability. The vitrinite reflectance ($R_o$) values vary from 2.2% to 3.8% (revised from Wang YM et al., 2021) and the peak temperatures of rock-eval pyrolysis ($T_{max}$) are between 320 and 590°C, which are now in the overmature stage.

The tectono-thermal history of different structural units in the Sichuan Basin varies, but the entire basin has gone through three stages: (1) before the Early Permian, it exhibited a stable low heat flow stage, with paleo-heat flow values ranging from 45 to 55 mW/m$^2$, which gradually decreased from the west to the east Sichuan Basin. (2) From the Early Permian to the Late Permian, affected by the thermal effect of the Emeishan mantle plume and the upwelling of the basement heat flow caused by lithospheric tension, the paleoheat flow values peaked in the Middle and Late Permian, with maximum values of 60–115 mW/m$^2$. In the region, there was a gradual decrease in the paleoheat flow from the center of the Emeishan mantle plume to the outside. (3) Since the Early Triassic, heat flow has gradually decreased and is currently relatively low, ranging from 47 to 60 mW/m$^2$ (Fig. 5; Qiu NS et al., 2022).

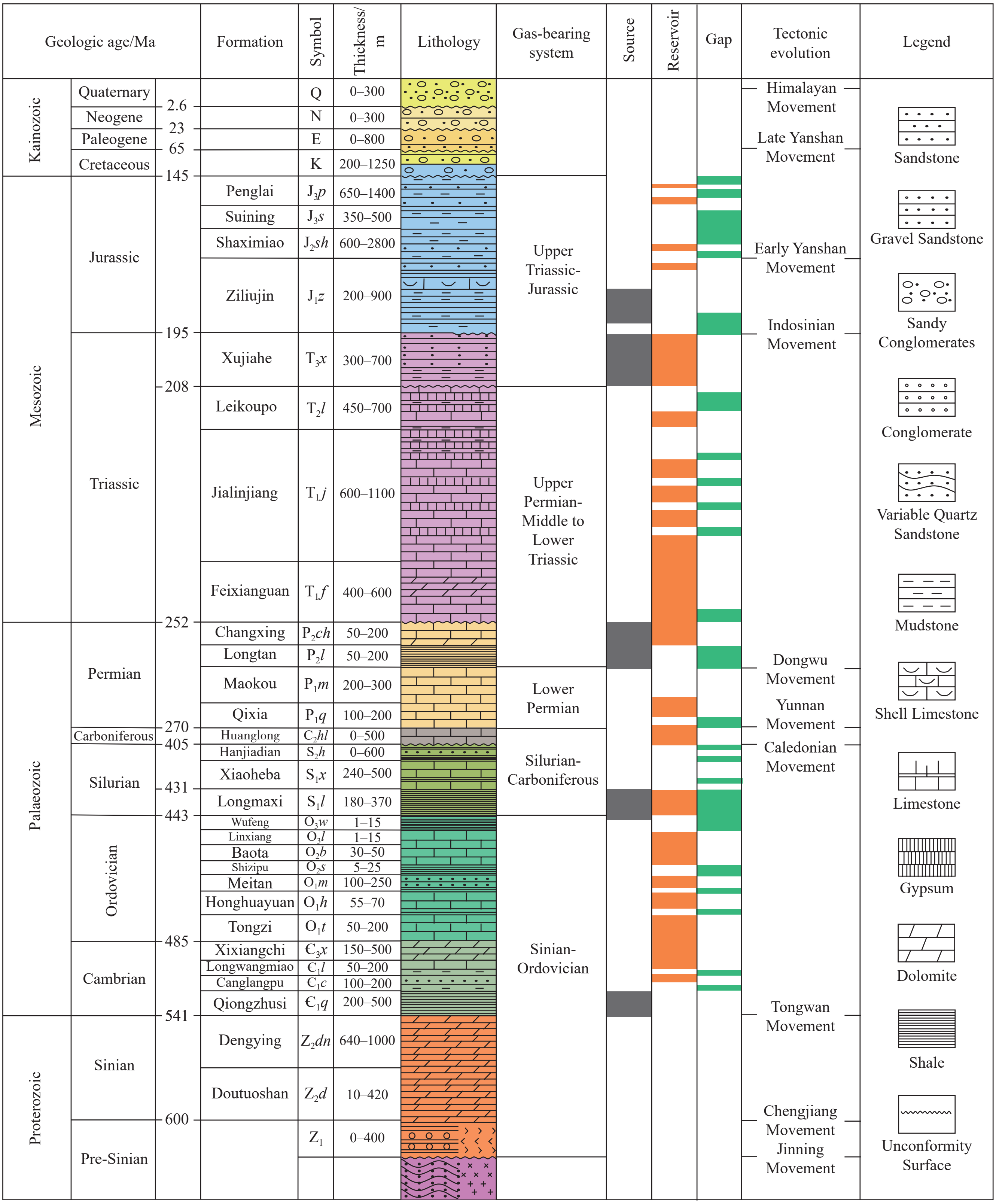


**Fig. 2.** Stratigraphic column map of the Sichuan Basin (revised from Zuo YH et al., 2024).

## 3. Methods and parameters

### *3.1. Methods*

The basin simulation software used in this manuscript is the BasinMod series software provided by Platte River Associates, Inc., in the United States (including BasinMod 1D, BasinView, and BasinFlow software). This software is widely used to examine sedimentary basin structural thermal systems and oil and gas reservoir dynamics and is currently among the most reliable basin simulation software packages (Baniasad A et al., 2021). In this work, BasinMod 1D

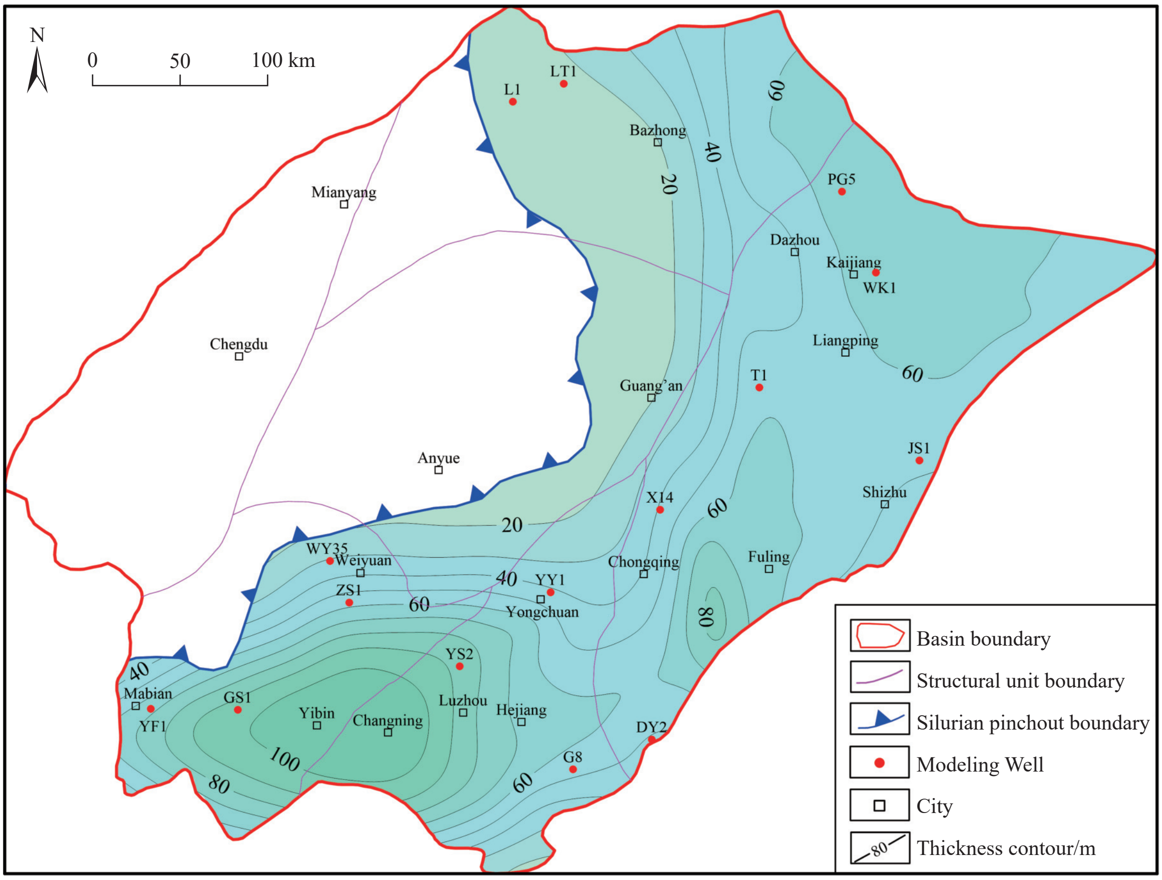


**Fig. 3.** Source rock thickness of the Lower Silurian Longmaxi Formation in the Sichuan Basin (revised from Hu ZQ et al., 2020; Wang YM et al., 2021).

software was initially utilized to constrain the tectono-thermal history. By integrating parameters such as geology, geochemistry, and paleothermometer data, a three-dimensional geological model of the Sichuan Basin was subsequently developed, utilizing the thicknesses of various strata and source rocks. Additionally, BasinView basin modeling software was used to explore the maturity evolution and hydrocarbon generation history of the Longmaxi Formation. The hydrocarbon generation rate of the Longmaxi Formation was subsequently calculated by the BasinFlow software. Finally, on the basis of the results of the maturity evolution and hydrocarbon generation history, combined with the thickness, TOC, and tectono-thermal history, the hydrocarbon evolution of the Longmaxi Formation during key geological periods was revealed. During modeling, the hydrocarbon generation kinetics model used the Easy% $R_o$ model (Sweeney JJ and Burnham AK, 1990). This model is widely used in the field of hydrocarbon generation kinetics, and the prediction accuracy for $R_o$ is also quite high. It is one of the most reliable hydrocarbon generation kinetic models at present (Qiu NS et al., 2022).

### *3.2. Parameters*

In basin modeling, numerous fundamental parameters are essential, and as exploration and geological knowledge increase, more basic parameters are obtained, and the greater the number of constraining parameters used in the model, the more reliable the simulation results are. For the basin modeling reported in this paper, the required basic parameters include geological parameters, geochemical parameters of the source rock, and thermal parameters. The geological parameters include the thickness, erosion amount, stratum stratification, and lithology of each stratum. The stratigraphic isopach map and erosion amount of each layer in the Sichuan Basin were obtained from the fourth oil and gas resource evaluation by PetroChina. The rock thermal conductivity (Table 1; Xu M et al., 2011), tectono-thermal history (Fig. 5; Qiu NS et al., 2022), and geochemical parameters of the source rocks were derived from previous studies (Nie HK et al., 2024; Hu ZQ et al., 2020; Wang YM et al., 2021). The stratigraphic stratification used actual values measured from boreholes, and the initial porosities and compaction coefficients were obtained through regression using the method of Slater and Christie (1980). The paleo-surface temperature in the simulation process was taken from the annual average temperature (15°C) of the Sichuan Basin (Yu Z, 2017). The key geological history periods of the modeling include: the end of the Caledonian Movement (405 Ma), the end of the Yunnan Movement (270 Ma), the end of the Dongwu Movement (256 Ma), the end of the Indosinian Movement (195 Ma), the end of the Yanshan Movement (100 Ma) and the present (0 Ma).

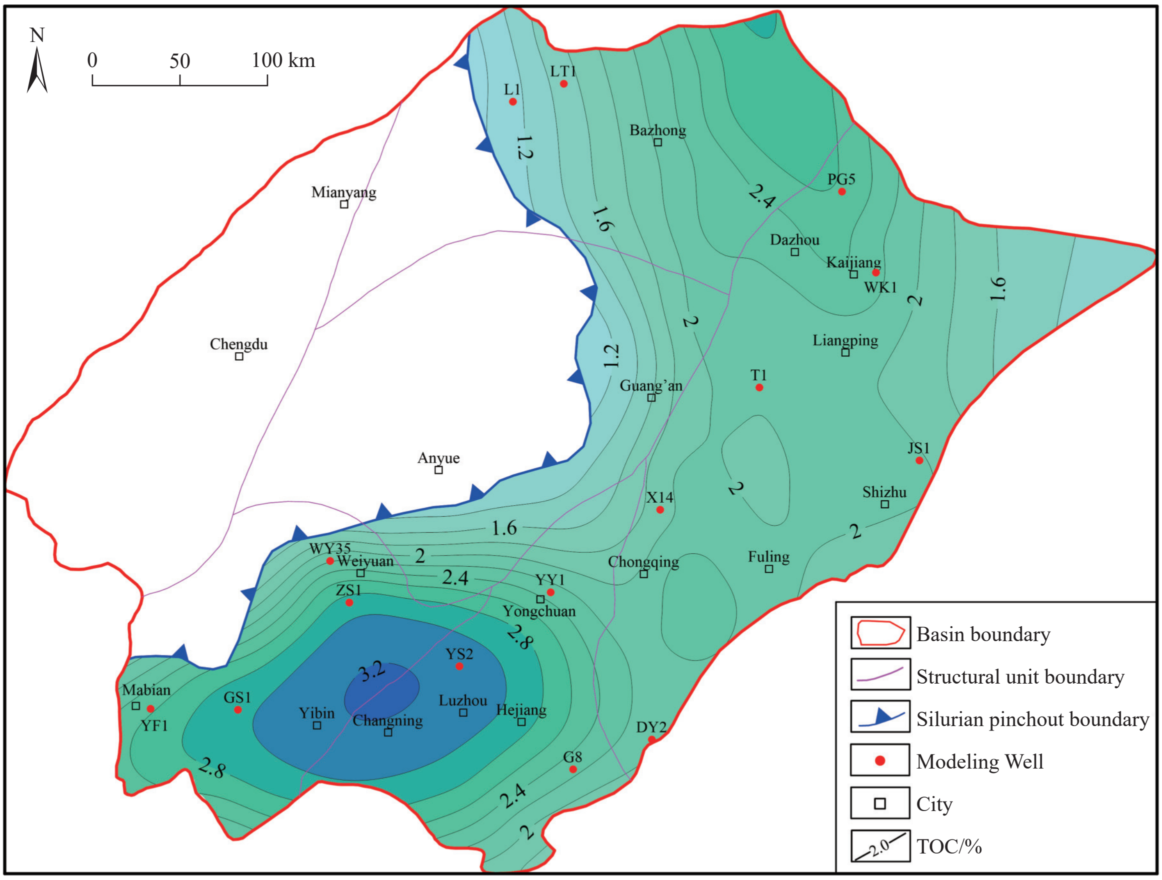


**Fig. 4.** Total organic carbon content (TOC) of the source rock of the Lower Silurian Longmaxi Formation in the Sichuan Basin (revised from Hu ZQ et al., 2020; Wang YM et al., 2021).

## 4. Results

### 4.1. Burial and thermal histories of typical wells

Reconstructing the burial history and thermal history of single wells is not only the basis for recovering the tectono-thermal history of a basin but also a verification tool to ensure the rationality of models during simulations of the maturity and hydrocarbon generation histories (Qiu NS et al., 2022). The measured and modeled values of $R_o$ were used for fitting and corrections, with a high degree of fit, indicating that the modeling results were correct.

Owing to the influence of the Caledonian Movement, the western and central Sichuan Basin experienced strong erosion, and most areas lacked Silurian–Carboniferous strata. Therefore, no research has been conducted on the Longmaxi Formation in the western and central Sichuan Basin. During the modeling, 15 typical wells were selected from the northern, eastern, southwestern, and southern Sichuan Basin to reconstruct the burial history and thermal history (Fig. 1; Table 2). The general parameters, including basin geological parameters and thermal indicators, were input into the BasinMod 1D software, and the burial and thermal histories were output during the reconstruction process via BasinMod 1D software. Taking 4 wells as an example, we show the input parameters of 15 modeling wells as follows (Table 3–6).

The source rock of the Lower Silurian Longmaxi Formation began to evolve with increasing burial depth in the Early Paleozoic. Owing to the uplift and erosion caused by the Caledonian tectonic process, the temperature decreased, and the evolution of the source rock stopped. During the Permian period, the strata were deeply buried again, and the temperature rapidly increased. By the Middle Cretaceous, the formation temperature had reached a maximum, and the degree of thermal evolution of the source rock had reached a maximum. After that, as the strata began to uplift, the temperature decreased, the level of maturity no longer increased, and the thermal evolution of the source rock stopped (Fig. 6).

### 4.2. Maturity history of source rock

The maturity history of source rocks refers to the maturity status and evolution process of source rocks at different stages during geological time (Qiu NS et al., 2021). This history is the basis for analyzing the development and migration evolution of hydrocarbon kitchens in a region (Qiu NS et al., 2021; Karg H and Sauerer B, 2022; Zhang JZ et al., 2023). It is mainly controlled by the temperature evolution during geological periods, which in turn depends on the burial history of the strata and the tectono-thermal history of the basin. Therefore, on the basis of the burial history and tectono-thermal history, the temperature history of the strata was obtained to determine the maturity history of the source

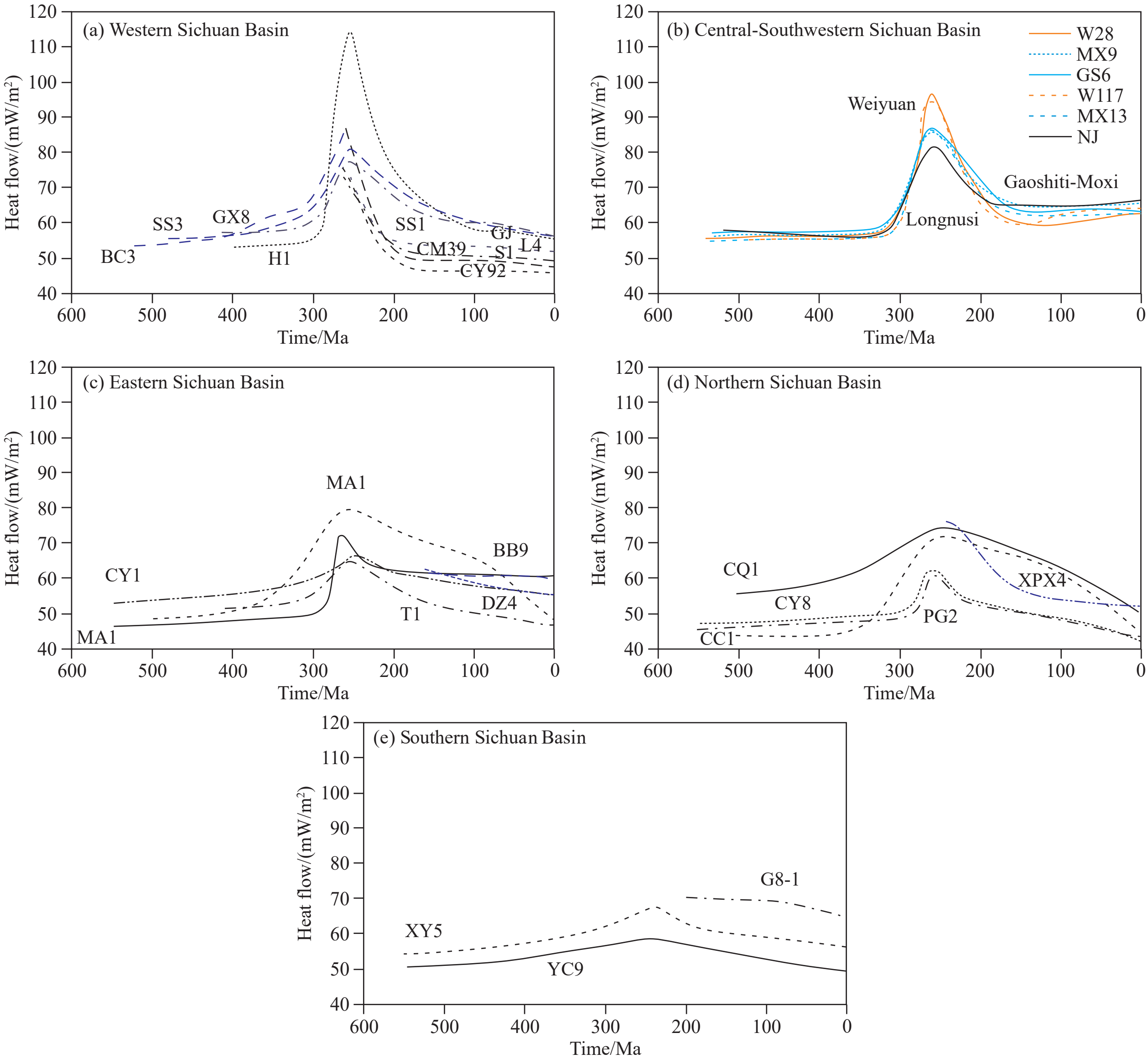


**Fig. 5.** Tectono-thermal histories of different structural units of the Sichuan Basin (Qiu NS et al., 2022). a–Western Sichuan Basin; b–Central-Southwestern Sichuan Basin; c–Eastern Sichuan Basin; d–Northern Sichuan Basin; e–Southern Sichuan Basin.

rock. The maturity evolution stages are divided into five stages: the immature stage ($R_o$ < 0.5%), low-maturity stage (0.5% ⩽ $R_o$ < 0.7%), medium-maturity stage (0.7% ⩽ $R_o$ < 1.0%), high-maturity stage (1.0% ⩽ $R_o$ < 1.3%), and over-maturity stage ($R_o$ ⩾ 1.3%). The high-maturity stage is the peak period of oil generation, and the over-mature stage is divided into the wet gas generation stage (1.3% ⩽ $R_o$ < 2.0%) and the dry gas generation stage ($R_o$ ⩾ 2.0%) (Zuo YH et al., 2017).

The simulation results indicate that the Longmaxi Formation was in the low-maturity stage, except that the central Sichuan Basin had not reached the hydrocarbon generation threshold at the end of the Caledonian Movement (Fig. 7a). During the Yunnan Movement, the maturity of the source rock in the central Sichuan Basin did not change significantly and was still in the immature stage. The maturity increased and was in the medium-maturity stage in most of the other areas (Fig. 7b). During the Dongwu Movement, the maturity increased greatly. The $R_o$ in the northern to southern Sichuan Basin reached 1.0%–1.3%, entering the high-maturity stage, which was the peak period of oil generation (Fig. 7c). During the Indosinian Movement, the maturity increased slightly, the whole region was generally still in the high-maturity stage, and the eastern part of the eastern Sichuan Basin reached the wet gas generation stage (Fig. 7d). During the Yanshan Movement, the maturity rapidly increased, the whole region entered the dry gas generation stage, and the $R_o$ values in the northern to southern Sichuan Basin reached a maximum of 3.6% (Fig. 7e). After that, the maturity has not increased (Fig. 7f).

### *4.3. Hydrocarbon generation history of source rock*

The hydrocarbon generation history of source rocks refers to the process and characteristics of hydrocarbon generation during geological time, which are usually characterized by changes in hydrocarbon generation intensity with geological time (Qiu NS et al., 2021). The hydrocarbon generation intensity is the amount of hydrocarbon generation per unit area of source rock, which can reflect the hydrocarbon generation ability of the source rock (Karg H and Littke R, 2020; Zeng JC et al., 2023). On the basis of the maturity evolution and geochemical parameters of the source rock, we used BasinView basin modeling software to restore the hydrocarbon generation intensities of the Longmaxi Formation in different geological periods, revealing the hydrocarbon generation process of the Longmaxi Formation.

At the end of the Caledonian Movement, the Longmaxi Formation in the Sichuan Basin began to generate hydrocarbons in the southern area. Nevertheless, the hydrocarbon generation intensity was weak, with a maximum of only $0.1\times10^6$ t/km$^2$ (Fig. 8a). During the Yunnan Movement, hydrocarbon generation occurred rapidly in the southern basin, and the maximum hydrocarbon generation intensity reached $3.0\times10^6$ t/km$^2$ in the Changning area (Fig. 8b). During the Dongwu Movement, the hydrocarbon generation intensity increased rapidly, and the generation range further expanded. The hydrocarbon generation centers were located mainly in the Yibin-Changning-Luzhou, Fuling, and Shizhu areas. The hydrocarbon generation intensity in the Yibin-Changning-Luzhou area was greater, reaching a maximum of $6.0\times10^6$ t/km$^2$, and the maximum intensity in the Fuling and Shizhu areas reached $2.0\times10^6$ t/km$^2$ (Fig. 8c). During the Indosinian Movement, the northern Sichuan Basin began to generate hydrocarbons, while the hydrocarbon generation intensity did not change much across the whole basin (Fig. 8d). During the Yanshan Movement, the hydrocarbon generation intensity significantly increased, and the entire region generated oil and gas. The hydrocarbon generation intensity in the Yibin-Changning-Luzhou area increased rapidly, with a maximum of $7.5\times10^6$ t/km$^2$; the hydrocarbon generation intensity in the Fuling area reached $3.5\times10^6$ t/km$^2$; and the Liangping-Kaijiang area also generated hydrocarbons rapidly, with a maximum intensity of $3.5\times10^6$ t/km$^2$ (Fig. 8e). After that, the source rock no longer generated hydrocarbons (Fig. 8f).

**Table 1. Rock thermal conductivity for strata in the Sichuan Basin (Xu M et al., 2011).**

| Stratum | Lithology | Sample numbers | Thermal conductivity (W/m·K) | Average value±standard deviation (W/m·K) |
|---|---|---|---|---|
| Jurassic | Sandstone | 29 | 1.827–3.773 | 2.70±0.52 |
| | Mudstone | 24 | 2.004–3.153 | 2.50±0.26 |
| | Limestone | 7 | 2.15–3.65 | 2.68±0.50 |
| Upper Triassic Xujiahe Formation | Sandstone | 34 | 2.244–4.99 | 3.46±0.65 |
| | Mudstone | 6 | 1.798–3.142 | 2.44±0.48 |
| top and Lower Triassic | Sandstone | 5 | 2.576–4.164 | 3.62±0.57 |
| | Mudstone | 1 | 3.118 | 3.12 |
| | Dolomite | 71 | 1.905–5.547 | 3.50±0.67 |
| | Limestone | 23 | 1.966–4.636 | 2.64±0.57 |
| | Anhydrite | 3 | 3.463–3.753 | 3.60±0.12 |
| Permian | Sandstone | 1 | 2.335 | 2.34 |
| | Mudstone | 4 | 1.694–3.331 | 2.36±0.60 |
| | Dolomite | 5 | 2.364–3.246 | 2.91±0.36 |
| | Limestone | 8 | 1.742–2.934 | 2.42±0.35 |
| Carboniferous | Limestone | 1 | 2.216 | 2.22 |
| Silurian | Mudstone | 7 | 2.064–2.795 | 2.46±0.30 |
| | Limestone | 16 | 1.955–2.632 | 2.38±0.20 |
| | Dolomite | 4 | 2.237–3.378 | 2.64±0.46 |
| Ordovician | Limestone | 2 | 2.199–2.302 | 2.25±0.05 |
| Cambrian | Mudstone | 8 | 2.157–2.868 | 2.58±0.25 |
| | Dolomite | 2 | 4.585–4.638 | 4.61±0.03 |
| Sinian | Dolomite | 20 | 3.311–4.696 | 4.01±0.36 |

### *4.4. Hydrocarbon kitchen evolution of the Longmaxi Formation*

The parameters used to characterize hydrocarbon kitchens mainly include the maturity, hydrocarbon generation intensity (or hydrocarbon generation amount), and hydrocarbon expulsion intensity (or hydrocarbon expulsion amount) (Yang MH et al., 2021; Rossello EA et al., 2022). In practical work,

**Table 2. Structural unit division, burial and thermal histories modeling wells in the Sichuan Basin.**

| Structural units | Modeling wells |
|---|---|
| Northern Sichuan Basin | L1, LT1 |
| Eastern Sichuan Basin | PG5, WK1, T1, X14, JS1, DY2 |
| Southern Sichuan Basin | G8, YS2, YY1 |
| Southwestern Sichuan Basin | ZS1, GS1, YF1, WY35 |

**Table 3. Input data for modeling of depositional and erosional events of Well GS1.**

| Formation | Lithology[a] | Deposition age (Ma) | | Erosion age (Ma) | | Denudation thickness (m) | Top (m) | Bottom (m) | Thickness (m) |
|---|---|---|---|---|---|---|---|---|---|
| | | From | To | From | To | | | | |
| J | Sandstone: 2%, Siltstone: 6%, Shale: 80%, Limestone: 12% | 195 | 100 | 100 | 0 | 2658 | 0 | 1731 | 1731 |
| $T_3x$ | Sandstone: 45%, Siltstone: 10%, Shale: 45% | 208 | 195 | | | | 1731 | 2033 | 302 |
| $T_{1\text{-}2}$ | Shale: 3%, Limestone: 42%, Dolomite: 28%, Evaporite: 27% | 252 | 209 | 209 | 208 | 635 | 2033 | 3143 | 1110 |
| P | Shale: 5%, Limestone: 95% | 270 | 252 | | | | 3143 | 3816 | 673 |
| C | Shale: 30%, Limestone: 70% | 405 | 270 | | | | 3816 | 4236 | 420 |
| S | Siltstone: 20%, Shale: 70%, Limestone: 10% | 443 | 407 | 407 | 405 | 230 | 4236 | 4411 | 175 |
| O | Shale: 25%, Limestone: 75% | 485 | 443 | | | | 4411 | 4970 | 559 |
| Є | Siltstone: 13%, Shale: 6%, Dolomite: 81% | 541 | 485 | | | | 4970 | 5787 | 817 |

[a] Formation lithology is obtained from logging data

**Table 4. Input data for modeling of depositional and erosional events of Well PG5.**

| Formation | Lithology [a] | Deposition age (Ma) | | Erosion age (Ma) | | Denudation thickness (m) | Top (m) | Bottom (m) | Thickness (m) |
|---|---|---|---|---|---|---|---|---|---|
| | | From | To | From | To | | | | |
| J | Sandstone: 2%, Siltstone: 6%, Shale: 80%, Limestone: 12% | 195 | 100 | 100 | 0 | 3471 | 0 | 2385 | 2385 |
| $T_3x$ | Sandstone: 45%, Siltstone: 10%, Shale: 45% | 208 | 195 | | | | 2385 | 2874 | 489 |
| $T_{1\text{-}2}$ | Limestone: 45%, Dolomite: 28%, Evaporite: 27% | 252 | 209 | 209 | 208 | 803 | 2873 | 4796 | 1923 |
| P | Shale: 5%, Limestone: 95% | 270 | 252 | | | | 4805 | 5508 | 703 |
| C | Shale: 30%, Limestone: 70% | 405 | 270 | | | | 5509 | 5865 | 356 |
| S | Siltstone: 18%, Shale: 70%, Limestone: 12% | 443 | 407 | 407 | 405 | 326 | 5516 | 5523 | 7 |
| O | Shale: 35%, Limestone: 65% | 485 | 443 | | | | 6431 | 6667 | 236 |
| Є | Siltstone: 62%, Shale: 12%, Dolomite: 26% | 541 | 485 | | | | 6667 | 7520 | 853 |

[a] Formation lithology is obtained from logging data.

**Table 5. Input data for modeling of depositional and erosional events of Well G8.**

| Formation | Lithology [a] | Deposition age (Ma) | | Erosion age (Ma) | | Denudation thickness (m) | Top (m) | Bottom (m) | Thickness (m) |
|---|---|---|---|---|---|---|---|---|---|
| | | From | To | From | To | | | | |
| J | Sandstone: 2%, Siltstone: 16%, Shale: 80%, Limestone: 2% | 195 | 100 | 100 | 0 | 2725 | 0 | 1533 | 1533 |
| $T_3x$ | Sandstone: 40%, Siltstone: 10%, Shale: 50% | 208 | 195 | | | | 1533 | 1720 | 187 |
| $T_{1\text{-}2}$ | Limestone: 52%, Dolomite: 28%, Evaporite: 20% | 252 | 209 | 209 | 208 | 700 | 1720 | 2970 | 1250 |
| P | Shale: 5%, Limestone: 95% | 270 | 252 | | | | 2970 | 3498 | 528 |
| C | Shale: 30%, Limestone: 70% | 405 | 270 | | | | 3498 | 3854 | 356 |
| S | Siltstone: 18%, Shale: 72%, Limestone: 10% | 443 | 407 | 407 | 405 | 134 | 3854 | 4450 | 596 |
| O | Shale: 33%, Limestone: 67% | 485 | 443 | | | | 4450 | 4968 | 518 |
| Є | Siltstone: 42%, Shale: 16%, Dolomite: 42% | 541 | 485 | | | | 4968 | 6593 | 1625 |

[a] Formation lithology is obtained from logging data.

**Table 6. Input data for modeling of depositional and erosional events of Well L1.**

| Formation | Lithology [a] | Deposition age (Ma) | | Erosion age (Ma) | | Denudation thickness (m) | Top (m) | Bottom (m) | Thickness (m) |
|---|---|---|---|---|---|---|---|---|---|
| | | From | To | From | To | | | | |
| J | Siltstone: 16%, Shale: 84% | 195 | 100 | 100 | 0 | 1522 | 0 | 3433 | 3433 |
| $T_3x$ | Sandstone: 45%, Siltstone: 10%, Shale: 45% | 208 | 195 | | | | 3433 | 4160 | 727 |
| $T_{1\text{-}2}$ | Limestone: 45%, Dolomite: 30%, Evaporite: 25% | 252 | 209 | 209 | 208 | 346 | 4160 | 6059 | 1899 |
| P | Shale: 60%, Limestone: 40% | 270 | 252 | | | | 6059 | 6651 | 592 |
| C | Shale: 32%, Limestone: 68% | 405 | 270 | | | | 6652 | 6856 | 204 |
| S | Siltstone: 21%, Shale: 70%, Limestone: 9% | 443 | 407 | 407 | 405 | 390 | 6856 | 7094 | 238 |
| O | Shale: 35%, Limestone: 65% | 485 | 443 | | | | 7094 | 7236 | 142 |
| Є | Siltstone: 60%, Shale: 15%, Dolomite: 25% | 541 | 485 | | | | 7237 | 8414 | 1177 |

[a] Formation lithology is obtained from logging data.

the hydrocarbon generation intensity center and its distribution range in a specific geological period are commonly used to characterize hydrocarbon kitchens (Pang XQ et al., 2015). Hydrocarbon kitchens with low hydrocarbon generation intensities cannot form oil and gas reservoirs with industrial value. Medium-sized and small oil and gas fields can only be found in areas with hydrocarbon generation intensities greater than $1.0\times10^6$ t/km$^2$, and large oil and gas fields can be found in areas with hydrocarbon generation intensities greater than $2.0\times10^6$ t/km$^2$. No industrial oil or gas reservoirs have been found in areas with hydrocarbon generation intensities less than $0.45\times10^6$ t/km$^2$ (Jin ZJ et al., 2003). Therefore, on the basis of the results of the source rock thickness, organic carbon content, tectono-thermal history and maturity history, this paper takes a hydrocarbon generation intensity of $2.0\times10^6$ t/km$^2$ as the lower limit, delineates the locations of effective hydrocarbon kitchens, and reveals the migration evolution laws for hydrocarbon kitchens in the key geological stage of the Lower Silurian Longmaxi Formation.

From the end of the Caledonian Movement to the end of the Yunnan Movement, the source rock of the Longmaxi Formation in the Sichuan Basin entered the hydrocarbon generation threshold. The source rocks in the Yibin-Changning-Luzhou area are thick, with a maximum thickness of 100 m and a high TOC of 3.2%. This stage reached the medium-maturity stage; thus, hydrocarbon kitchens began to develop (HCK Ⅰ), with a maximum intensity of $3.0\times10^6$ t/km$^2$ (Fig. 9a). From the end of the Yunnan Movement to the end of the Dongwu Movement, HCK Ⅰ continued to develop, and the hydrocarbon generation range expanded. The

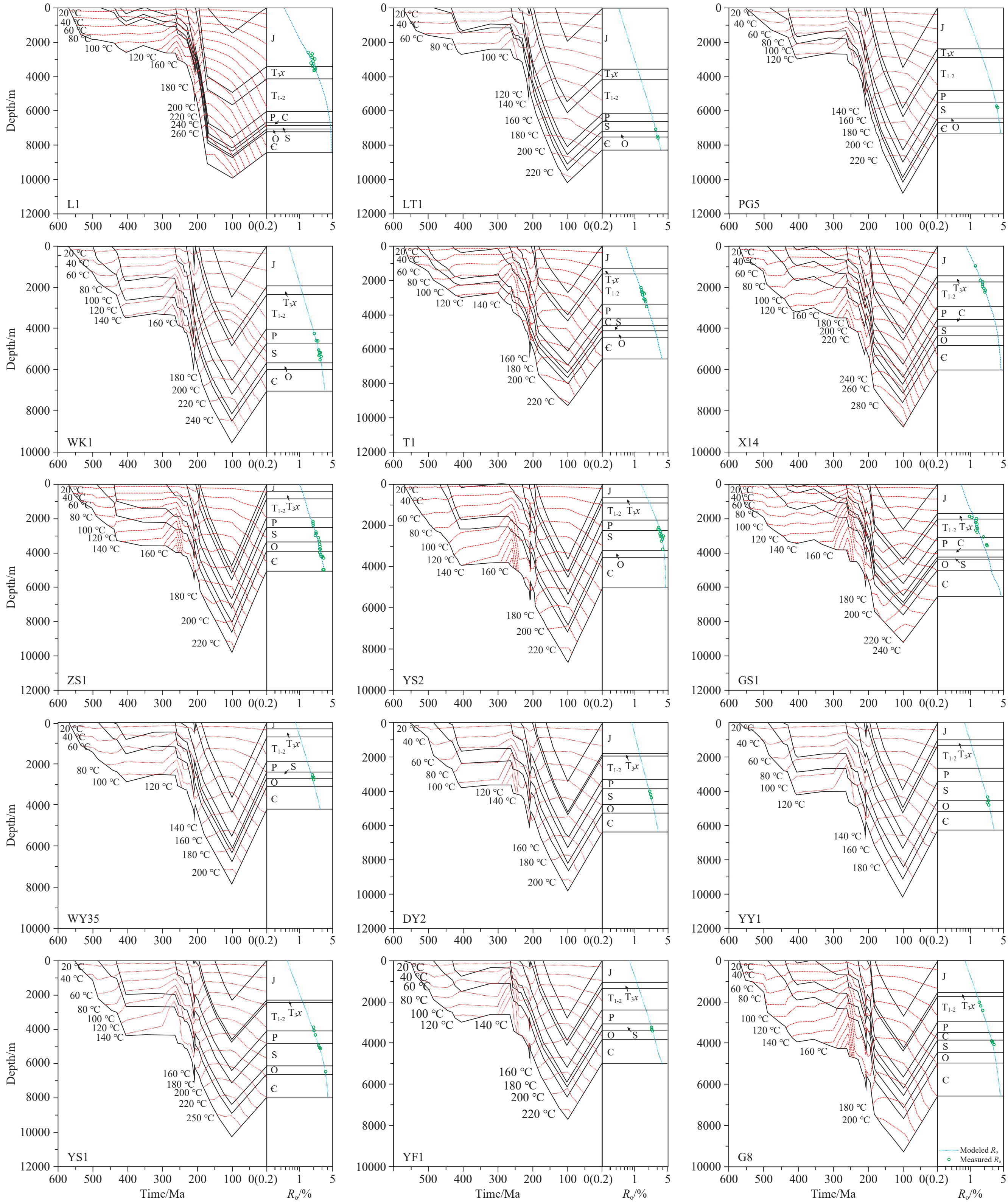


**Fig. 6.** Burial and thermal histories of typical wells in the Sichuan Basin. The green "○" means measured vitrinite reflectance ($R_o$) datum, and the broken blue line means modeled result in the right chart. Among them, the modeling well L1 and LT1 is located in the Northern Sichuan Basin. PG5, WK1, T1, X14, JS1, and DY2 wells are located in the Eastern Sichuan Basin. G8, YS2, and YY1 wells are located in the Southern Sichuan Basin. GS1, ZS1, YF1, and WY35 wells are located in the Southwestern Sichuan Basin (as shown in Fig. 1).

source rock entered the high-maturity stage, which was the peak period of oil generation, generated large amounts of oil, and the maximum hydrocarbon generation intensity in this hydrocarbon kitchen reached 5.0×10$^6$ t/km$^2$. Moreover, a new hydrocarbon kitchen formed in the Fuling area (HCK Ⅱ), with a maximum thickness of 80 m and a high TOC of 2.0%; in the high-maturity and high-oil generation stages, the maximum hydrocarbon generation intensity in HCK Ⅱ

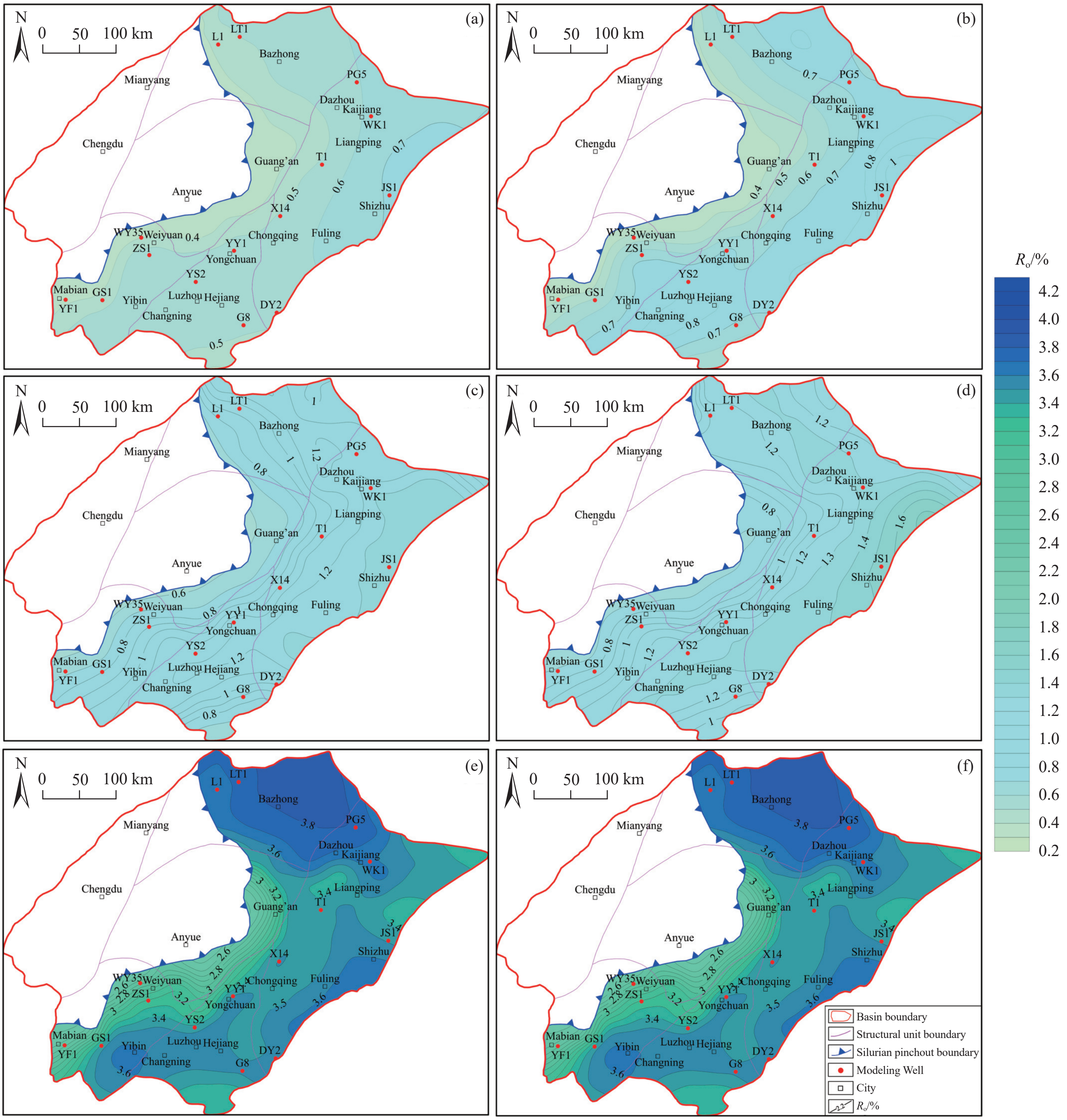


**Fig. 7.** Maturity evolution of top surface of the Lower Silurian Longmaxi ormation in key geological periods. a–End of the Caledonian Movement. b–End of the Yunnan Movement. c–End of the Dongwu Movement. d–End of the Indosinian Movement. e–End of the Yanshan Movement. f–Present.

reached $2.5×10^6$ t/km$^2$ (Fig. 9b). From the end of the Dongwu Movement to the end of the Indosinian Movement, the maturity of the source rock did not change significantly, and the hydrocarbon generation capacity was weak, with underdeveloped hydrocarbon kitchens (Fig. 9c). From the end of the Indosinian Movement to the end of the Yanshan Movement, HCK Ⅰ continued to develop, and the hydrocarbon generation range expanded further. The source rock entered the dry gas generation stage, and the kerogen not only generated oil but also generated natural gas. In addition to kerogen cracking, many crude oils were cracked to generate natural gas. HCK Ⅱ migrated northward, forming a new hydrocarbon kitchen in the Kaijiang-Liangping area (HCK Ⅲ). Owing to the large thickness of the source rock in this area, with a maximum thickness of more than 60 m and a high TOC of up to 2.6%, the highest maturity of the source rock reached 3.8%, and it had entered the dry gas generation stage. The newly formed hydrocarbon kitchen had an

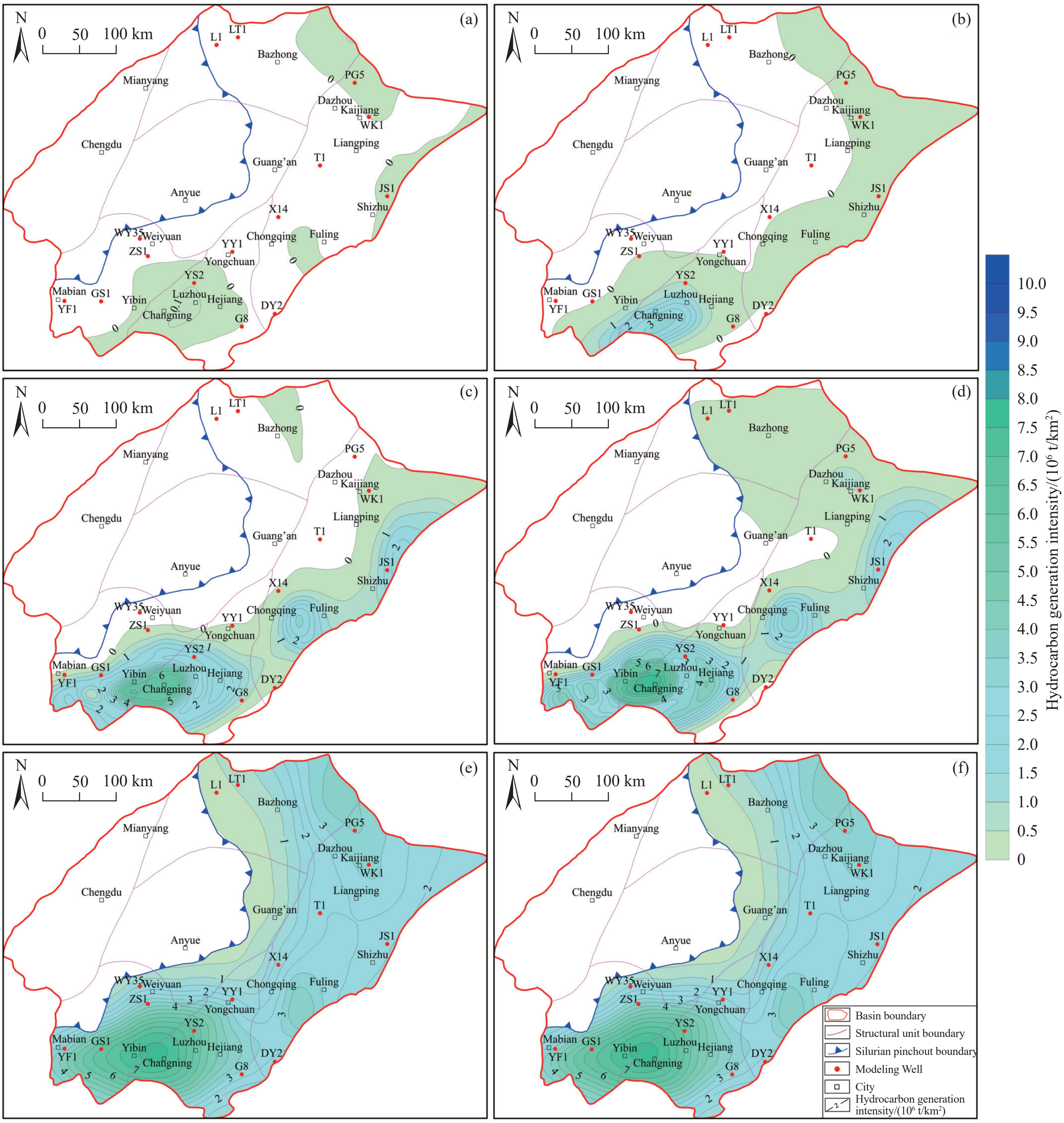


**Fig. 8.** Hydrocarbon generation intensity of the Lower Silurian Longmaxi Formation in key geological periods. a–End of the Caledonian Movement. b–End of the Yunnan Movement. c–End of the Dongwu Movement. d–End of the Indosinian Movement. e–End of the Yanshan Movement. f– Present.

extensive range and high hydrocarbon generation intensity, with a maximum hydrocarbon generation intensity of $3.0\times10^6$ t/km$^2$ (Fig. 9d). Afterward, as the strata began to rise and the temperature decreased, the thermal evolution of the Longmaxi Formation in the Sichuan Basin stopped, and hydrocarbon generation stopped.

To further clarify the main hydrocarbon generation periods and stages of the Longmaxi Formation and whether hydrocarbon generation was dominated by oil or gas, based on the hydrocarbon generation intensity during the key geological periods, BasinFlow modeling software was used to simulate the oil and gas generation rates and their amounts in the Longmaxi Formation and to clarify the specific hydrocarbon generation stages. The source rock of the Longmaxi Formation experienced two main stages of oil generation: the Yunnan Movement-the end of the Dongwu Movement (Late Carboniferous-Early Permian) and the early stage of the Early Yanshan Movement (Early Jurassic) (Fig. 10).

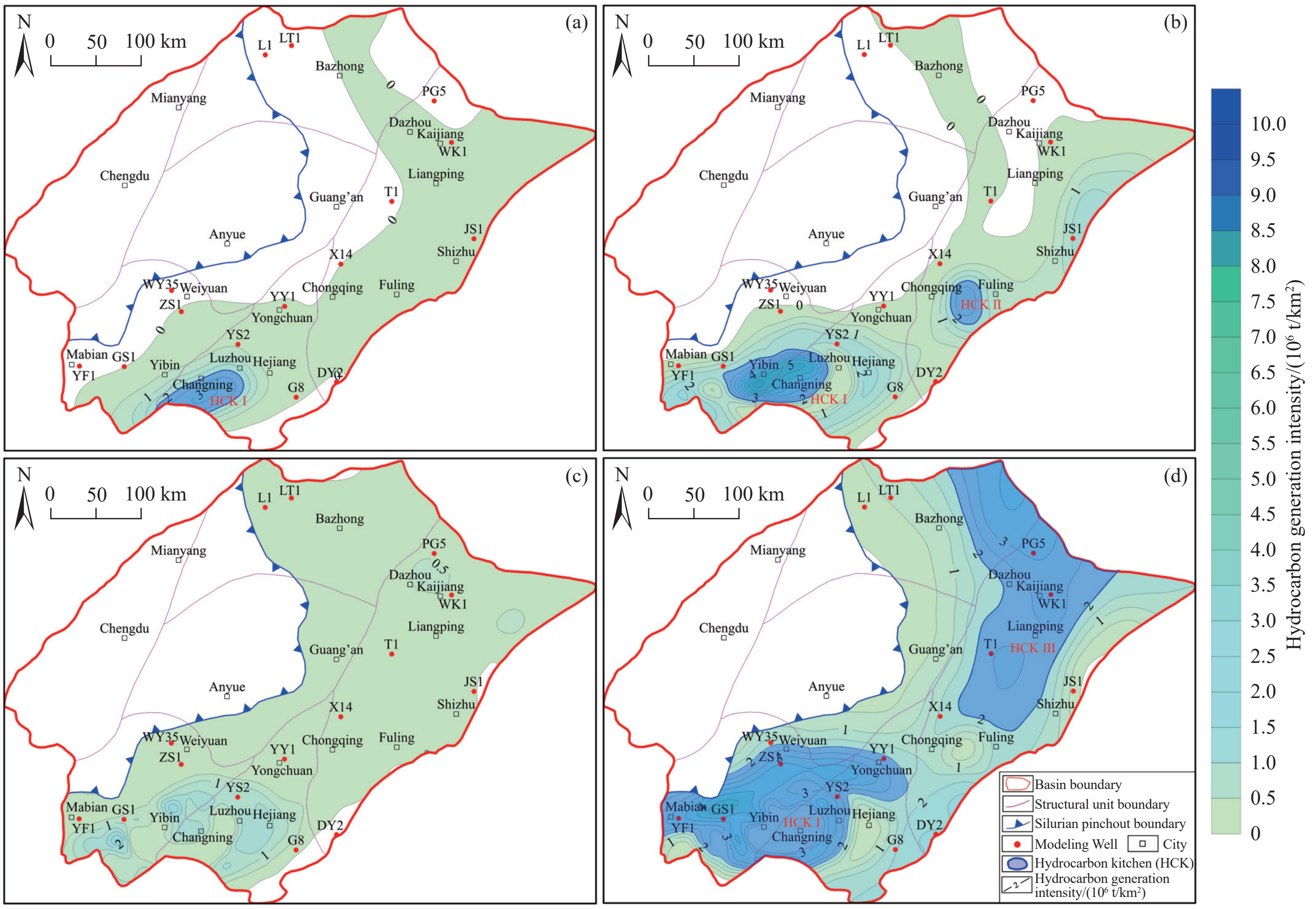


**Fig. 9.** Hydrocarbon kitchen evolution of the Lower Silurian Longmaxi Formation in different stages. a–End of the Caledonian Movement to End of the Yunnan Movement. b–End of the Yunnan Movement to End of the Dongwu Movement. c–End of the Dongwu Movement to End of the Indosinian Movement. d–End of the Indosinian Movement to End of the Yanshan Movement. Based on the results of the source rock thickness, organic carbon content, tectono-thermal history and maturity history, this paper takes the hydrocarbon generation intensity of $2.0\times10^6$ t/km$^2$ as the lower limit, delineates the location of effective hydrocarbon kitchens. HCK Ⅰ–the Hydrocarbon kitchen in the Yibin-Changning-Luzhou areas; HCK Ⅱ–the Hydrocarbon kitchen in the Fuling area; HCK Ⅲ–the hydrocarbon kitchen in the Kaijiang-Liangping areas.

It has gone through three stages of gas generation, namely, the Yunnan Movement-the end of the Dongwu Movement (Late Carboniferous-Early Permian), the end of the Indosinian Movement (Early Triassic), and the early stage of the Early Yanshan Movement (Early Jurassic). The accumulative oil generation amount was $5722.4\times10^8$ t, and the gas generation amount was $1527.6\times10^8$ m$^3$ (Fig. 11). Both periods were dominated by oil generation and were supplemented by gas generation. However, as geological time progresses, the burial depth of the strata continues to increase, the temperature increases, and the maturity of the source rock increases. The crude oil that was generated during the Early Yanshan Movement had a lighter composition than that generated during the Dongwu Movement, and the contents of condensate oil, wet gas, and dry gas increased.

## 5. Discussion

### *5.1. Contribution of hydrocarbon kitchen evolution to gas accumulation*

Overall, the main hydrocarbon generation period of the Longmaxi Formation had two stages, and three hydrocarbon kitchens formed. That is, in the early stage (Yunnan Movement-end of the Dongwu Movement), two major hydrocarbon kitchens developed in the Yibin-Changning-Luzhou area (HCK Ⅰ) and Fuling area (HCK Ⅱ). In the late stage (early stage of the Early Yanshan Movement), HCK Ⅰ developed further, and HCK Ⅱ migrated northward to form a new hydrocarbon kitchen in the Kaijiang-Liangping area (HCK Ⅲ). During geological time, the different degrees of migration evolution of hydrocarbon kitchens have noticeable controlling effects on gas accumulations and distributions.

During the Caledonian Movement, under the regional uplifts of the Sichuan Basin, the central-western Sichuan area was greatly uplifted to form the Leshan-Longnüsi paleo-uplift (Ma XH et al., 2019). In addition, paleo-depressions formed around the paleo-uplift. A large area of thick argillaceous source rock of the Longmaxi Formation is distributed in the southern to eastern Sichuan Basin (Ma XH et al., 2019; Liu SG et al., 2020). Notably, paleo-uplifts are typically situated in elevated sections of the crust, serving as favorable units for the migration and accumulation of oil and gas. Conversely,

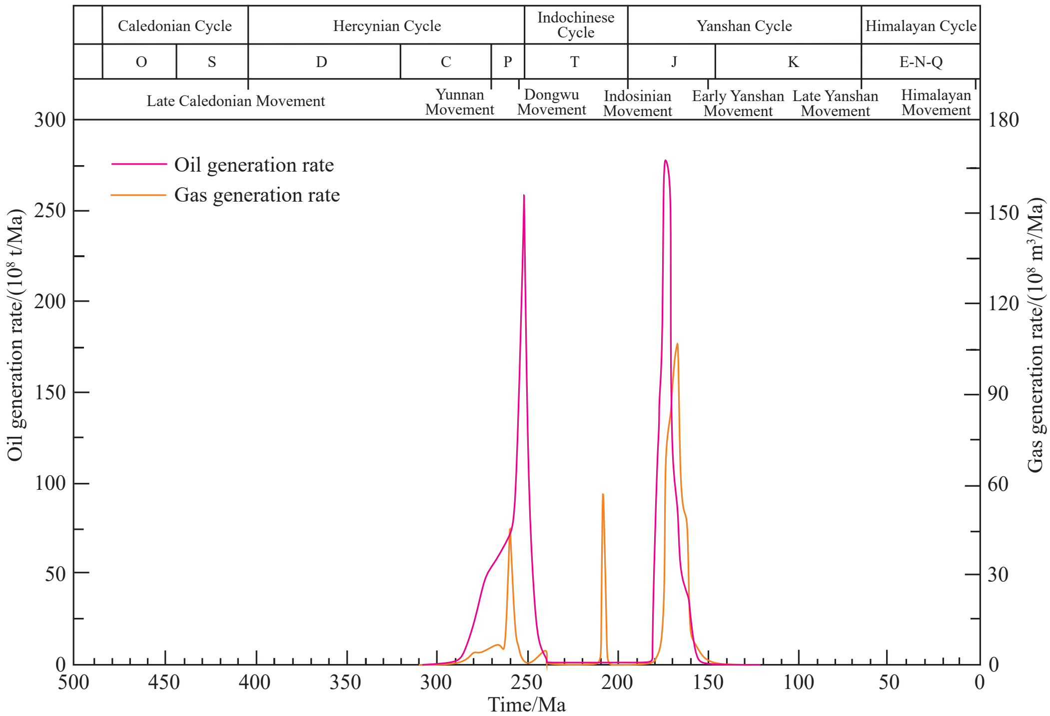


**Fig. 10.** Hydrocarbon generation rate of the source rock of the Longmaxi Formation in the Sichuan Basin.

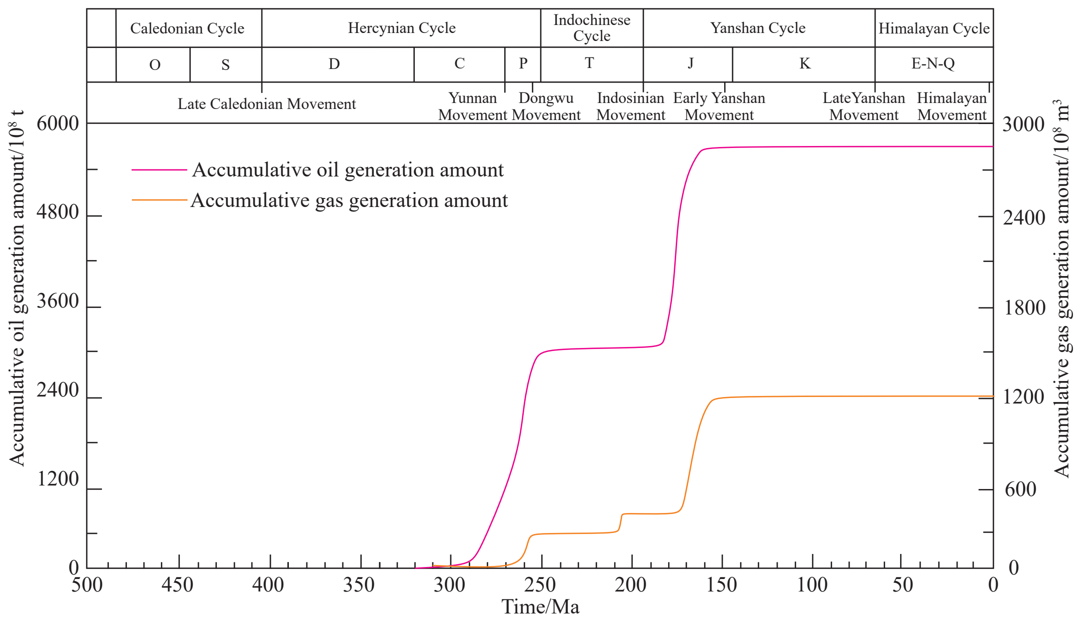


**Fig. 11.** Accumulated hydrocarbon generation amount of the source rock of the Longmaxi Formation in the Sichuan Basin.

paleo-depressions reside in areas of subsiding crust, potentially functioning as development zones for source rocks and reservoir formations. These two geological features are interconnected and are mutually influential in terms of their geological structures (Liu SG et al., 2021). During the Yunnan Movement to the end of the Dongwu Movement, with the deep burial of strata, the temperature increased and was affected by the thermal maturity effect of the Emeishan mantle plume and the upwelling of basement heat flow caused by lithospheric tension (Qiu NS et al., 2022; Feng QQ et al., 2025). The thermal evolution of the source rock increased rapidly, entering the period of peak oil generation. HCK Ⅰ and HCK Ⅱ generated large amounts of oil, and the hydrocarbon generation intensity reached $6.0\times10^6$ t/km$^2$ in HCK Ⅰ. At this time, although the reservoir of the Carboniferous Huanglong Formation had already been deposited, the trap had not yet formed (Xu GS et al., 2011; Ma XH et al., 2019). Thus, it was difficult for the crude oil that was generated in this stage to accumulate effectively to form paleo-reservoirs (Fig. 12a). At the early stage of the early Yanshan Movement, the strata were deeply buried again, and the temperature increased rapidly. The thermal

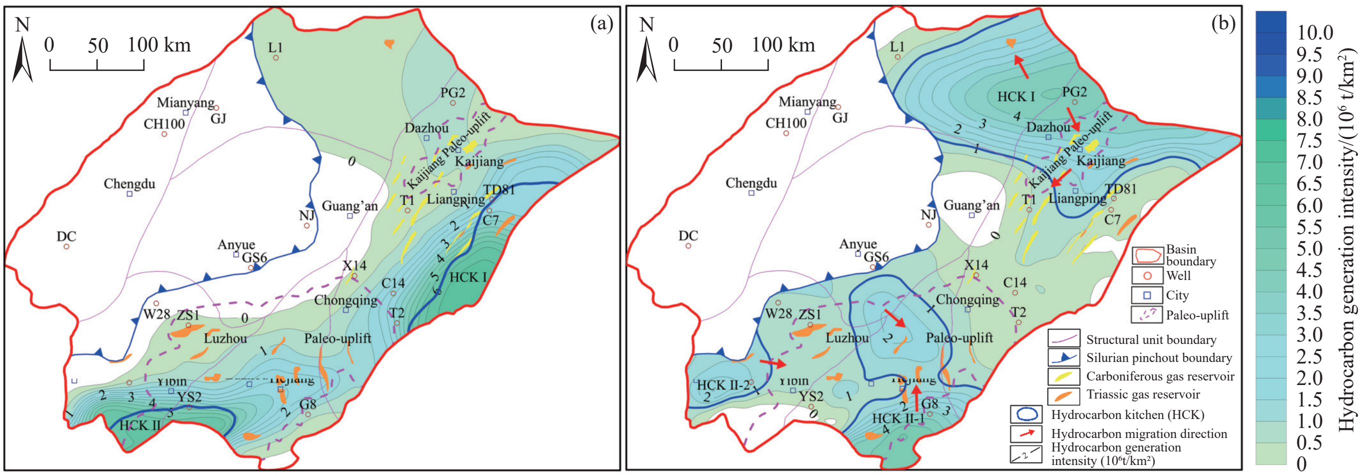


**Fig. 12.** The two main hydrocarbon generation processes of the hydrocarbon kitchens of the Longmaxi Formation and their relationship with gas accumulation. (a) The Yunnan Movement to the end of the Dongwu Movement. (b) The early stage of the Early Yanshan Movement. HCK Ⅰ–the Hydrocarbon kitchen in the Yibin-Changning-Luzhou areas; HCK Ⅱ–the Hydrocarbon kitchen in the Fuling area; HCK Ⅲ–the Hydrocarbon kitchen in the Kaijiang-Liangping areas.

maturity evolution of the Longmaxi Formation accelerated again, and the whole area entered the dry gas generation stage. The kerogen not only generated oil but also generated large amounts of natural gas. The hydrocarbon generation intensities reached $4.0\times10^6$ t/km$^2$ in HCK Ⅰ and $3.5\times10^6$ t/km$^2$ in HCK Ⅲ. In addition to the influence of the maturity evolution of the source rock, this transition was also affected by the Luzhou paleo-uplift and the Kaijiang paleo-uplift that formed during the Indosinian period (Liu SG et al., 2021). At this time, in addition to the Carboniferous reservoirs, the Permian and Triassic reservoirs had also been deposited, and under the control of the Luzhou paleo-uplift and Kaijiang paleo-uplift, multiple types of structural traps had already developed (Nie HK et al., 2017; Ma XH et al., 2019; Li SG et al., 2023). The large amounts of oil and gas (mainly oil supplemented by gas) that were generated from the two hydrocarbon kitchens migrated to the high parts of the paleo-uplifts and accumulated in traps to form paleo-oil reservoirs (Fig. 12b). When the reservoir temperature reaches 150–160°C, crude oil begins to crack and generate natural gas (Zhu GY et al., 2018), forming paleo-gas reservoirs. Large amounts of asphalt in reservoirs can be used as evidence for the formation of natural gas by the thermal cracking of crude oil in paleo-oil reservoirs (Li H et al., 2023; Ma XH et al., 2019). In addition, the gas mixture generated from kerogen at the late cracking stage and secondary cracking of residual crude oil could provide a natural gas source for the Longmaxi shale gas reservoir, which is consistent with the results of the gas composition and isotope analysis of the Fuling shale gas reservoir (Liu QY et al., 2018). Combined with the migration and evolution characteristics of the hydrocarbon kitchens, the location of the paleo-uplifts, and the large- and medium-sized gas fields that have been discovered, in the early stage of the early Yanshan Movement, there was an excellent spatiotemporal matching relationship that was composed of high structural belts, a large number of hydrocarbon generation scales, high-quality reservoirs, and good traps, providing an essential basis for the formation of large-scale natural gas reservoirs.

### *5.2. Favorable areas for exploration*

The fundamental concept that the distribution of oil and gas reservoirs is controlled by hydrocarbon kitchens has become an important theory to guide oil and gas exploration (Jin ZJ et al., 2003; Fairhurst B et al., 2021; Evenick JC et al., 2023). After analyzing the distribution characteristics of hydrocarbon reservoirs in Chinese oil and gas basins, Pang XQ et al. (2015) reported that over 95% of oil and gas reservoirs (in terms of quantity and reserves) are distributed within and around the main hydrocarbon generation ranges of hydrocarbon kitchens or within radii that are twice those of hydrocarbon kitchens, and areas that are closer to the center of hydrocarbon kitchens have greater probabilities of oil and gas accumulations. The natural gas in the Sichuan Basin has originated mainly from the crude oil cracking of paleo-oil reservoirs, which is a consensus view (Liu et al., SG 2020; Huang SP et al., 2023; Zheng ZY et al., 2023). The paleo-oil reservoirs were synchronously cracked to form paleo-gas reservoirs and then synchronously transformed to form the present gas reservoirs. The areas of paleo-oil reservoir development reveal areas that are favorable for exploration. On the basis of this understanding, combined with the location and evolution characteristics of hydrocarbon kitchens, tectonic movements, and the locations of discovered large- and medium-sized gas fields, potential areas for the development of paleo-oil reservoirs in the Sichuan Basin have been delineated, including the Luzhou paleo-oil reservoir and Kaijiang paleo-oil reservoir (Fig. 13).

For the areas with favorable exploration prospects for conventional natural gas reservoirs that are located in the area of the Luzhou paleo-oil reservoir, the Permian strata overlying the Longmaxi Formation served as reservoirs or cap rocks (Ma XH et al., 2019; Liu SG et al., 2020). The oil and gas

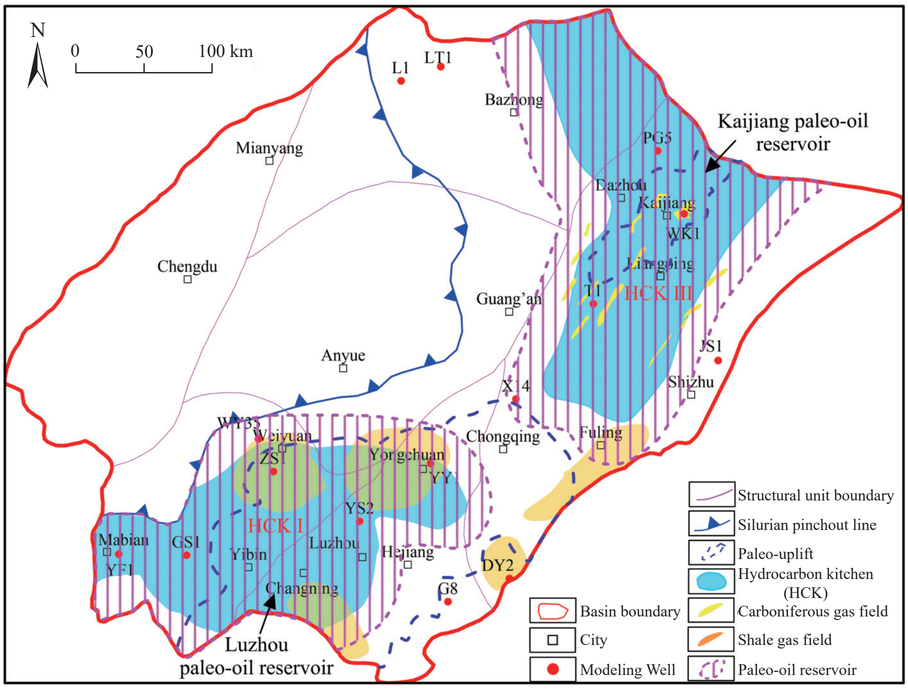


**Fig. 13.** Hydrocarbon kitchens and paleo-oil reservoir development potential areas of the Lower Silurian Longmaxi Formation in the Sichuan Basin. HCK Ⅰ–the Hydrocarbon kitchen in the Yibin-Changning-Luzhou areas; HCK Ⅲ–the Hydrocarbon kitchen in the Kaijiang-Liangping areas.

generated by the Longmaxi Formation in HCK Ⅰ could have accumulated in the Permian reservoir of the Luzhou paleo-uplift to form the Luzhou paleo-oil reservoir. In the potential areas of the Kaijiang paleo-oil reservoir, the oil and gas generated by the Longmaxi Formation in HCK Ⅲ mainly migrated to the Carboniferous reservoir combination in the eastern Sichuan Basin and the Permian reservoir combination in the northern Sichuan Basin, forming the Kaijiang paleo-oil reservoir (Ma XH et al., 2019; Liu SG et al., 2020). When the reservoir temperature reached 150–160 °C, the crude oil in the paleo-oil reservoirs cracked to generate large amounts of natural gas (Zhu GY et al., 2018), which were mixed with the natural gas generated by late kerogen cracking (Nie HK et al., 2024). On the one hand, it provided a gas source for the conventional natural gas reservoirs, and on the other hand, it also supplied gas for the shale gas of the Longmaxi Formation. Therefore, for exploration efforts to replace the conventional natural gas produced in the Sichuan Basin, the focus should be on finding large- and medium-sized natural gas reservoirs in the high-quality strata of the Luzhou paleo-oil reservoir and Kaijiang paleo-oil reservoir and their surroundings. The Longmaxi Formation shale can be used as both a source rock and a reservoir, and the shale gas reservoir conditions are good. The two paleo-oil reservoir development areas and their surroundings are also favorable areas for shale gas reservoir exploration.

## 6. Conclusions

(i) The maturity evolution of the Longmaxi Formation source rock in different structural areas exhibits both common traits and differences. All regions entered the oil generation threshold at the end of the Late Caledonian Movement, with an increase in maturity during the Yunnan Movement. During the Dongwu Movement, the maturity evolution accelerated, and reached the dry gas generation stage during the Yanshan Movement, followed by no further increases in maturity. Moreover, owing to differences in the tectono-thermal history, burial history, and source rock characteristics, the maturity evolution in different structural areas was quite different.

(ii) The source rock of the Longmaxi Formation began to generate hydrocarbons extensively during the Yunnan Movement. During the Dongwu Movement, the range of hydrocarbon generation further expanded, and the hydrocarbon generation centers were located mainly in the Yibin-Changning-Luzhou, Fuling and Shizhu areas, with the maximum hydrocarbon generation intensity reaching $6.0\times10^6$ t/km$^2$ in the Yibin-Changning-Luzhou area. During the Indosinian Movement, the hydrocarbon generation intensity did not change significantly. During the Yanshan Movement, it increased significantly, and the hydrocarbon generation intensity in the Yibin-Changning-Luzhou area reached $7.5\times10^6$ t/km$^2$. Since then, hydrocarbon generation has stopped.

(iii) The main hydrocarbon generation period of the Longmaxi Formation consisted of two stages, three hydrocarbon kitchens were formed, and all of them mainly generated oil, with natural gas as a supplement. During the Yunnan Movement to the end of the Dongwu Movement, two major hydrocarbon kitchens developed in the Yibin-Changning-Luzhou area (HCK Ⅰ) and Fuling area (HCK Ⅱ). During the early stage of the early Yanshan Movement, HCK Ⅰ developed further, and HCK Ⅱ migrated northward to form a new hydrocarbon kitchen in the Kaijiang-Liangping area (HCK Ⅲ). The generated oil and gas migrated to the high parts of the paleo-uplifts and accumulated in traps to form the Luzhou and Kaijiang paleo-oil reservoirs.

(ⅳ) The identification and migration evolution of hydrocarbon kitchens are key topics in oil and gas exploration research. This research can provide direction for predicting areas with oil and gas potential and establishing well locations. The natural gas in the Sichuan Basin has originated mainly from the crude oil cracking of paleo-oil reservoirs, and the distribution of hydrocarbon kitchens reveals the development areas of paleo-oil reservoirs, thereby revealing potential areas for oil and gas exploration. Therefore, for the replacement exploration of conventional natural gas in the Sichuan Basin, the focus should be on finding large and medium-sized natural gas reservoirs in the high-quality strata of the Luzhou paleo-oil reservoir, Kaijiang paleo-oil reservoir, and their surroundings. The Longmaxi Formation shale can be used as both a source rock and a reservoir, and the shale gas reservoir conditions are good. The two paleo-oil reservoir development areas and their surroundings are also favorable areas for shale gas reservoir exploration.

## Acknowledgments

This work was funded by the National Natural Science Foundation of China (Grant No. 42372172), the Sichuan Science and Technology Program (Grant Nos. 23NSFSC1211, 2024NSFSC0083), and the Tianfu Yongxing Laboratory Science and Technology Research Program (Grant No. 2023KJGG13). At the same time, we would like to express our sincere gratitude to the editor in chief and two reviewers for their assistance in providing valuable suggestions in the manuscript.

## Author Contributions

Jia-zhen Zhang carried out the basin simulation and wrote the original draft. Chang-cheng Wang and Yin-hui Zuo conceived of the presented idea, writing-review and funding acquisition. Xin-guo Duan and Wen-ming Huang provided the research methods. Mei-hua Yang and Jian-cheng Zeng conducted the investigation and data curation. All authors discussed the results and contributed to the final manuscript.

## Declaration of competing interest

The authors declare no conflicts of interest.

## References

Agyeman SD, Lin BQ. 2023. The influence of natural gas (De)regulation on innovation for climate change mitigation: Evidence from OECD countries. Environmental Impact Assessment Review, 98, 106961. doi: 10.1016/j.eiar.2022.106961.

Baniasad A, Littke R, Froidl F, Grohmann S, Soleimany B. 2021. Quantitative hydrocarbon generation and charge risk assessment in the NW Persian Gulf: A 3D basin modeling approach. Marine and Petroleum Geology, 126, 104900. doi: 10.1016/j.marpetgeo.2021.104900.

Chen L, Chen X, Tan XC, Zheng J, Yang Y, Jing C, Zhou H, Wang GX. 2023. Factors controlling organic matter accumulation in the Longmaxi Formation shale, Changning area, South Sichuan Basin. Geomechanics and Geophysics for Geo-Energy and Geo-Resources, 9(1), 89. doi: 10.1007/s40948-023-00585-5.

da Silva VO, Relva SG, Mondragon M, Mendes AB, Nishimoto K, Peyerl D. 2023. Building options for the Brazilian pre-salt: A technical-economic and infrastructure analysis of offshore integration between energy generation and natural gas exploration. Resources Policy, 81, 103305. doi: 10.1016/j.resourpol.2023.103305.

Demaison G. 1984. The generative basin concept. Petroleum Geochemistry and Basin Evaluation. American Association of Petroleum Geologists. doi: 10.1306/m35439c1.

de Almeida dos Reis MAA, Damasceno AC, Roriz CED, Korenchendler AL, da Silva AM, da Silva Praxedes E, Silva VG. 2023. Source rock evaluation from rock to seismic data: An integrated machine-learning-based work flow and application in the Brazilian presalt (santos basin). Minerals, 13(9), 1179. doi: 10.3390/min13091179.

Evenick JC. 2023. Evaluating the lacustrine Shahejie Formation source rock potential in the Bohai Bay Basin using a simplified regional basin model. Journal of Natural Gas Geoscience, 8(4), 279–291. doi: 10.1016/j.jnggs.2023.07.001.

Fairhurst B, Ewing T, Lindsay B. 2021. West Texas (Permian) super basin, United States: Tectonics, structural development, sedimentation, petroleum systems, and hydrocarbon reserves. AAPG Bulletin, 105(6), 1099–1147. doi: 10.1306/03042120130.

Feng QQ, Qiu NS, Fu XD, Borjigin T, Luo QY, Zhu CQ. 2025. Permian thermal pulse event in Southwestern China and its resource and environment effects. Global and Planetary Change, 246, 104722. doi: 10.1016/j.gloplacha.2025.104722.

Fritz RD, Mitchell JR. 2021. The anadarko “super” basin: 10 key characteristics to understand its productivity. AAPG Bulletin, 105(6), 1199–1231. doi: 10.1306/03242120082.

Guo XS, Hu DF, Huang RC, Wei ZH, Duan JB, Wei XF, Fan XJ, Miao ZW. 2020. Deep and ultra-deep natural gas exploration in the Sichuan Basin: Progress and prospect. Natural Gas Industry, 40(5), 1–14 (in Chinese with English abstract).

He ZL, Nie HK, Hu DF, Jiang TX, Wang RY, Zhang YY, Zhang GR, Lu ZY. 2020. Geological problems in the effective development of deep shale gas: A case study of Upper Ordovician Wufeng-Lower Silurian Longmaxi Formations in Sichuan Basin and its periphery. Acta Petrolei Sinica, 41(4), 379–391 (in Chinese with English abstract).

Hou ZY, Niu XY, Yu ZY, Chen W. 2024. Spatiotemporal evolution and market dynamics of the international liquefied natural gas trade: A multilevel network analysis. Energies, 17(1), 228. doi: 10.3390/en17010228.

Hu ZQ, Zhu T, Du W, Wu J, Wang GP. 2021. Fine grained sedimentary research and shale lithology mapping. Beijing: Geological Publishing House (in Chinese).

Huang SP, Jiang QC, Jiang H, Tang QS, Zeng FY, Lu WH, Hao CG, Yuan M, Wu Y. 2023. Genetic and source differences of gases in the Middle Permian Qixia and Maokou formations in the Sichuan Basin, SW China. Organic Geochemistry, 178, 104574. doi: 10.1016/j.orggeochem.2023.104574.

Jin ZJ., Zhang YW., Wang J. 2003. Hydrocarbon Accumulation Mechanisms and Oil/Gas Distribution. Petroleum Industry Press, Beijing (in Chinese).

Karg H, Littke R. 2020. Tectonic control on hydrocarbon generation in the northwestern Neuquén Basin, Argentina. AAPG Bulletin, 104(10), 2173–2208. doi: 10.1306/05082018171.

Karg H, Sauerer B. 2022. Thermal maturity assessment of marine source rocks integrating Raman spectroscopy, organic geochemistry and petroleum systems modeling. International Journal of Coal Geology, 264, 104131. doi: 10.1016/j.coal.2022.104131.

Li H, Zheng MJ, Li YJ, Long H, Geng C, Li CH, Liu T, Pu HG, Tang H. 2023. Oil and gas distribution law and exploration and development prospects of Jialingjiang Formation in Luzhou Indosinian paleouplift of the Sichuan Basin. Natural Gas Industry, 43(7), 10–21 (in Chinese with English abstract).

Liu, K. , Zhang, C. , 2022. Elementary Geochemical Characteristics and Sedimentary Tectonic Evolution of Longmaxi Formation in Southern Sichuan Basin, China. Fresenius Environmental Bulletin 31(3), 2700−2707.

Liu QY, Jin ZJ, Wang XF, Yi JZ, Meng QQ, Wu XQ, Gao B, Nie HK, Zhu DY. 2018. Distinguishing kerogen and oil cracked shale gas using H, C-isotopic fractionation of alkane gases. Marine and Petroleum Geology, 91, 350–362. doi: 10.1016/j.marpetgeo.2018.01.006.

Liu SG, Deng B, Sun W, Song JM, Jiao K, Ye YH, Xie GL. 2020. May Sichuan basin be a super petroliferous basin? Journal of Xihua University (Natural Science Edition), 39(5), 20–35 (in Chinese with English abstract).

Liu SG, Yang Y, Deng B, Zhong Y, Wen L, Sun W, Li ZW, Jansa L, Li JX, Song JM, Zhang XH, Peng HL. 2021. Tectonic evolution of the Sichuan basin, southwest China. Earth-Science Reviews, 213, 103470. doi: 10.1016/j.earscirev.2020.103470.

Ma XH, Yang Y, Wen L, Luo B. 2019. Distribution and exploration direction of medium- and large-sized marine carbonate gas fields in Sichuan Basin, SW China. Petroleum Exploration and Development, 46(1), 1–15. doi: 10.1016/S1876-3804(19)30001-1.

Moghaddam H, Kunst RM. 2023. The role of natural gas in mitigating greenhouse gas emissions: The environmental kuznets curve hypothesis for major gas-producing countries. Sustainability, 15(5), 4266. doi: 10.3390/su15054266.

Nie HK, Jin ZJ, Ma X, Liu ZB, Lin T, Yang ZH. 2017. Dispositional characteristics of Ordovician Wufeng Formation and Silurian Longmaxi Formation in Sichuan basin and its adjacent areas. Petroleum Research, 2(3), 233–246. doi: 10.1016/j.ptlrs.2017.01.003.

Nie HK, Zhang JC, Jin ZJ, Liu QY, Li SJ, Dang W, Li P, Bian RK, Sun CX, Zhang K, Su HK. 2024. Enrichment mechanism of marine shale gas—a case study of the Wufeng Formation-Longmaxi Formation in the Sichuan basin, SW China. Acta Geologica Sinica, 98(3), 975–991 (in Chinese with English abstract). doi: 10.19762/j.cnki.dizhixuebao.2023278.

Pang XQ, Bao ZD, Cai CF, Chen JF, Chen JP, Chen JQ, Dong YX, Fu LG. 2015. Hydrocarbon distribution threshold and accumulation areas prediction. Beijing: Science Press (in Chinese).

Qi L, Wang HY, Shi ZS, Zhou TQ, Li GZ, Sun SS, Cheng F. 2023. Mineralogical and geochemical characteristics of the deeply buried Wufeng–Longmaxi shale in the southern Sichuan basin, China: Implications for provenance and tectonic setting. Minerals, 13(12), 1502. doi: 10.3390/min13121502.

Qiu NS, Chang J, Zhu CQ, Liu W, Zuo YH, Xu W, Li D. 2022. Thermal regime of sedimentary basins in the Tarim, Upper Yangtze and North China Cratons, China. Earth-Science Reviews, 224, 103884. doi: 10.1016/j.earscirev.2021.103884.

Qiu NS, Liu W, Fu XD, Li WZ, Xu QC, Zhu CQ. 2021. Maturity evolution of lower Cambrian qiongzhusi formation shale of the Sichuan basin. Marine and Petroleum Geology, 128, 105061. doi: 10.1016/j.marpetgeo.2021.105061.

Rossello EA, Cossey SPJ, Fernández G. 2021. The hydrocarbon potential of the offshore talara basin, Peru. Andean Geology, 49(1), 1–17. doi: 10.5027/andgeov49n1-3383.

Saputra W, Kirati W, Patzek T. 2021. Forecast of Economic Tight Oil and Gas Production in Permian Basin. Energies, 15(1), 43. doi: 10.3390/en15010043.

Sclater JG, Christie PAF. 1980. Continental stretching—explanation of post-mid-cretaceous subsidence of central north sea basin: ABSTRACT. AAPG Bulletin, 64(5), 781–782. doi: 10.1306/2f919201-16ce-11d7-8645000102c1865d.

Shabani F, Amini A, Tavakoli V, Chehrazi A, Gong CR. 2023. 3D basin and petroleum system modelling of the Early Cretaceous play in the NW Persian Gulf. Geoenergy Science and Engineering, 226, 211768. doi: 10.1016/j.geoen.2023.211768.

Smit DJ, Powell JB. 2023. Role of international oil companies in the net-zero emission energy transition. Annual Review of Chemical and Biomolecular Engineering, 14, 301–322. doi: 10.1146/annurev-chembioeng-092220-030446.

Strategic Research Center of Oil and Gasa Resources, Ministry of Land and Resources, 2016. Investigation and evolution and selection of favorable areas of the potential of shale gas resources in China. Beijing: Science Press.

Sweeney JJ, Burnham AK. 1990. Evaluation of a simple model of vitrinite reflectance based on chemical kinetics. AAPG Bulletin, 74, 1559–1570. doi: 10.1306/0c9b251f-1710-11d7-8645000102c1865d.

Tang X, Guo YC, Zhou TQ, Guo S. 2021. Distribution characteristics of nanopores and discriminant characteristics of sedimentary environment of the Longmaxi Formation in the southern Sichuan basin. Journal of Nanoscience and Nanotechnology, 21(1), 431–437. doi: 10.1166/jnn.2021.18741.

Thomas BM, Møller-Pedersen P, Whitaker MF, Shaw ND. 1985. Organic facies and hydrocarbon distributions in the Norwegian north sea. Petroleum Geochemistry in Exploration of the Norwegian Shelf. 1985. Dordrecht: Springer Netherlands, 3–26. doi: 10.1007/978-94-009-4199-1_1.

Tian XW., Sun YT., Yang DL., Wang YL., Peng HL., Ma K., Zhang XH., Wang H., Ye M., Xu L., Ren JB., Dou S., 2020. A Further Discussion on Source-Control Theory--By the Example of Marine Carbonate Gas Reservoir in the Sichuan Basin. Acta Geologica Sichuan 40(2), 410−415 (in Chinese with English abstract).

Veefkind JP, Serrano-Calvo R, de Gouw J, Dix B, Schneising O, Buchwitz M, Barré J, van der A RJ, Liu M, Levelt PF. 2023. Widespread frequent methane emissions from the oil and gas industry in the Permian basin. Journal of Geophysical Research: Atmospheres, 128(3), e2022JD037479. doi: 10.1029/2022jd037479.

Wang K, Hu SY, Li W, Liu W, Huang QY, Ma K, Shi SY. 2016. Depositional system of the Carboniferous Huanglong formation, eastern Sichuan basin: Constraints from sedimentology and geochemistry. Acta Geologica Sinica, 90(5), 1795–1808. doi: 10.1111/1755-6724.12817.

Wang YM., Li XJ., Dong DZ., Wang HY., Jin X., Sheng JJ., Qiu, Z. 2020. Geological characteristics of typical section of Silurian shale in Sichuan Basin and its surrounding areas. Beijing: Petroleum Industry Press (in Chinese).

Wei GQ, Xie ZY, Yang Y, Li J, Yang W, Zhao LZ, Yang CL, Zhang L, Xie WR, Jiang H, Li ZS, Li J, Guo JY. 2022. Formation conditions of Sinian–Cambrian large lithologic gas reservoirs in the north slope area of central Sichuan Basin, SW China. Petroleum Exploration and Development, 49(5), 963–976. doi: 10.1016/S1876-3804(22)60325-2.

Wu B. 2022. The sedimentary geochemical characteristics and geological significance of the Wufeng-Longmaxi Formation accumulation of organic matter black shale on the southeastern Sichuan basin, China. Geofluids, 2022, 1900158. doi: 10.1155/2022/1900158.

Xiao B, Liu SG, Li ZW, Ran B, Ye YH, Yang D, Li JX. 2021. Geochemical characteristics of marine shale in the Wufeng Formation–Longmaxi Formation in the northern Sichuan Basin, South China and its implications for depositional controls on organic matter. Journal of Petroleum Science and Engineering, 203, 108618. doi: 10.1016/j.petrol.2021.108618.

Xu GS, Xu YG, Liu SG, Yuan HF, Cao JF, Yang YH. 2011. Allegiance of four centers and pool-forming process of Carboniferous in Sichuan Basin of China. Journal of Chengdu University of

Technology (Science & Technology Edition), 38(4), 369–377 (in Chinese with English abstract).

Xu M, Zhu CQ, Tian YT, Rao S, Hu SB. 2011. Borehole temperature logging and characteristics of subsurface temperature in the Sichuan Basin. Chinese Journal of Geophysics, 54(4), 1052–1060 (in Chinese with English abstract).

Yang MH, Zuo YH, Zhang JZ, Wang CC, Zhou YS, Wang XJ, Zhang CF. 2021. Hydrocarbon kitchen evolution in the Early Cretaceous bayingebi 2 formation in the Chagan depression, yingen-ejinaqi basin, north Central China. ACS Omega, 6(18), 12194–12204. doi: 10.1021/acsomega.1c00944.

Yang Z, Zou CN, Gu ZD, Yang F, Li JR, Wang XN. 2022. Geological characteristics and main challenges of onshore deep oil and gas development in China. Advances in Geo-Energy Research, 6(3), 264–266. doi: 10.46690/ager.2022.03.09.

Yu Z. , 2017. Changes of Ground Temperature in Sichuan and Evaluation Model. Chengdu University of Technology (in Chinese with English abstract).

Zeng JC, Zuo YH, Zheng ZY, Zhang JZ, Ge JW, Song LK, Xiao Y, Zhao XM. 2023. Gas–source comparison and hydrocarbon generation and expulsion histories of the main source rocks of the Middle Jurassic shaximiao formation, western Sichuan basin. ACS Omega, 8(48), 46113–46126. doi: 10.1021/acsomega.3c07134.

Zhang JZ, Zuo YH, Yang MH, Huang WM, Xu L, Zheng ZY, Zeng JC. 2023. Hydrocarbon generation and expulsion histories of the upper Permian Longtan formation in the eastern Sichuan basin, southwest China. ACS Omega, 8(22), 19329–19340. doi: 10.1021/acsomega.3c00048.

Zhang NN, Wang JJ, Xue MH, Wang Q, Wu YP, Cao QC, Sun PL. 2024. Research on the security of natural gas supply and demand in China under the dual carbon target. Science Progress, 107(1), 368504231220851. doi: 10.1177/00368504231220851.

Zheng ZY, Zuo YH, Wen HG, Li DM, Luo Y, Zhang JZ, Yang MH, Zeng JC. 2023. Natural gas characteristics and gas-source comparisons of the Lower Triassic Feixianguan Formation, Eastern Sichuan Basin, China. Petroleum Science, 20(3), 1458–1470. doi: 10.1016/j.petsci.2023.02.005.

Zhu GY, Milkov AV, Chen FR, Weng N, Zhang ZY, Yang HJ, Liu KY, Zhu YF. 2018. Non-cracked oil in ultra-deep high-temperature reservoirs in the Tarim basin, China. Marine and Petroleum Geology, 89, 252–262. doi: 10.1016/j.marpetgeo.2017.07.019.

Zuo YH, Qiu NS, Zhang Y, Li CC, Li JP, Guo YH, Pang XQ. 2011. Geothermal regime and hydrocarbon kitchen evolution of the offshore Bohai Bay Basin, North China. AAPG Bulletin, 95(5), 749–769. doi: 10.1306/09271010079.

Zuo YH, Sun YG, Zhang LQ, Zhang C, Wang YC, Jiang GZ, Wang XG, Zhang T, Cui LQ. 2024. Geothermal resource evaluation in the Sichuan Basin and suggestions for the development and utilization of abandoned oil and gas wells. Renewable Energy, 225, 120362. doi: 10.1016/j.renene.2024.120362.

Zuo YH, Ye B, Wu WT, Zhang YX, Ma WX, Tang SL, Zhou YS. 2017. Present temperature field and Cenozoic thermal history in the Dongpu depression, Bohai Bay Basin, North China. Marine and Petroleum Geology, 88, 696–711. doi: 10.1016/j.marpetgeo.2017.08.037.